Modulation of T-cell apoptosis by small molecule compounds targeting the nuclear orphan receptor Nur77

Inauguraldissertation

zur

Erlangung der Würde eines Doktors der Philosophie

vorgelegt der

Philosophisch-Naturwissenschaftlichen Fakultät

der Universität Basel

von

Florian Marquardsen

aus Trier, Rheinland-Pfalz, Deutschland

Basel, 2018

Genehmigt von der Philosophisch-Naturwissenschaftlichen Fakultät
auf Antrag von

Prof. Dr. med. Christoph Hess (Fakultätsverantwortlicher)
Prof. Dr. med. Mike Recher (Dissertationsleiter)
Prof. Dr. med. Nina Khanna (Koreferentin)

Basel, den 26.06.2018

Prof. Dr. Martin Spiess (Dekan)

Table of content

List of Figures

List of Tables

1 Introduction

The adaptive immune system must ensure the homeostasis of its cell populations to avoid lymphoproliferation and exaggerated immune responses in order to prevent immune-dysregulatory disease. One way to guarantee adaptive immune cell homeostasis is to regulate and initiate adaptive immune cell death in the presence or absence of infection[1,2].

1.1 Regulated cell death in T-cells

The efficacy of the adaptive immune system, and of T-lymphocytes in particular, is based on a rapid clonal expansion of pathogen-specific T-cells. To ensure stable absolute T-cell numbers following clearance of an infection, controlled T-cell contraction has to occur *via* regulated cell death (RCD).

RCD is defined as an instantaneous and severe diminution of cells that are exposed to physical or biochemical stress factors[3,4]. RCD has been intensively investigated over the last decades. RCD maintains cellular homeostasis by eliminating useless, hyperactive and potentially dangerous or infected cells[5–8]. Also, RCD is of central importance for the maintenance of self-tolerance during the development of T-cells in the thymus by negative selection[9–11]. Furthermore, RCD enables dying cells to release intracellular molecules, so called damage associated molecular patterns (DAMPs) or alarmins, that can be sensed by surrounding cells in a paracrine manner[12–15].

Since cell death is associated with various morphological cellular changes, subtypes of RCD have been classified according to the morphological phenotypes. These are (1) type I cell death (apoptosis), (2) type II cell death (autophagy) and (3) type III cell death (necrosis)[16,17]. Recent research in RCD led to a new model of classifying these cell death cascades by the Nomenclature Committee on Cell Death (NCCD), that focuses on the signaling cascades, that are involved and responsible for initiation and execution of RCD. This new classification aims to achieve more accuracy by characterizing cell death according to genetic, biochemical, pharmacological and functional nature[3,17–21].

1.1.1 Re-stimulation induced *vs*. cytokine withdrawal induced RCD in T-cells

T-cell contraction following clonal expansion is controlled by two distinct forms of RCD[22]. An optimal T-cell expansion is achieved *via* a prolonged engagement of an antigen in context with the MHC complex on the antigen presenting cell (APC) *via* the highly specific T-cell receptor (TCR). In addition, co-stimulatory molecules such as CD28 are required to support optimal T-cell activation. T-cell expansion also requires rapid production of IL-2 and

expression of its respective surface receptor (CD25)[23]. Re-encountering of the cognate peptide by an activated antigen-specific T-cell may initiate T-cell apoptosis called re-stimulation induced cell death (RICD) or activation induced T-cell death (AICD)[24,25].

It is still not entirely clear, why the TCR ligation by pathogen-derived peptide may primarily promote survival and proliferation but may induce apoptosis upon subsequent TCR ligation[26,27]. However, it is commonly accepted, that RICD reflects an important and sensitive feedback threshold to effectively constrain an effector T-cell pool, depending on quantity and quality of the abundant antigen, the amount of growth factors and the cellular microenvironment[23]. During an adaptive immune response, abundance of antigen and levels of survival-associated cytokines, such as IL-2, IL-15 and IL-7, decrease following pathogen clearance. This withdrawal of cytokines *per se* may also induce cytokine withdrawal induced T-cell death (CWID)[28,29].

Both mechanisms (RICD and CWID) occur at different timepoints during the immune response and show different apoptosis kinetics *in vitro*.

1.1.2 *Extrinsic vs. intrinsic* T-cell apoptosis

T-cell RCD occurs *via* two signaling pathways that are not mutual exclusive[23,30]. Mitochondrial dysfunction induced by mitochondrial outer membrane permeabilization (MOMP) is the orchestrator of *intrinsic* apoptosis[31,32]. BAX, BAK and BOK are the only apoptosis regulator family (BCL-2) related proteins known so far that induce pores in the outer mitochondrial membrane[33–36]. BAX and BAK are inactive in physiological conditions but may be activated to induce MOMP by binding to pro-apoptotic proteins of the BCL-2 family[37–39]. These comprise the proteins NOXA and PUMA whose expression is mainly regulated by transcriptional activation, while BID expression is regulated post-translationally[40–45]. Negative regulators of BAX and BAK are the anti-apoptotic members of the BCL-2 family, comprising BCL-X_L, BCL-W and BFL-1. They mediate their apoptosis-inhibiting function by directly binding to the pro-apoptotic BCL-2 family members[46–48]. During *intrinsic* apoptosis, MOMP is followed by cytochrome C release from mitochondria into the cytoplasm where it binds to apoptosis peptidase activating factor 1 (APAF1) and pro-caspase 9[49]. This protein complex catalyzes the activation of the *intrinsic* initiator caspase 9[50]. Activated, proteolytically processed caspase 9 then catalyzes the proteolytic activation of the effector caspase 3 and caspase 7 that are responsible for the morphological and biochemical correlates of apoptosis, such as DNA fragmentation, phosphatidylserine exposure and the formation of apoptotic bodies due to membrane reorganization[18]. Another factor that is released from mitochondria during MOMP is DIABLO, also known as second mitochondrial activator of caspases (SMAC)[51–53]. Upon release into the cytoplasm, SMAC binds to members of the inhibitor of apoptosis proteins including XIAP (x-linked inhibitor of apoptosis) and inactivates

its anti-apoptotic function. XIAP stably binds to effector caspases and inhibits their proteolytic activation[54–56].

The *extrinsic* apoptosis pathway is activated by perturbations of the extracellular microenvironment. *Extrinsic* apoptosis is induced by binding of ligands to several death receptors on the cell surface. Death receptors comprise FAS (CD95), TNFα receptor 1 (TNFR1) and TRAIL receptors 1 and 2 (DR4 and DR5)[57]. Ligation of death receptors lead to intracellular conformational changes allowing formation of death-inducing signaling complexes (DISC). DISC bind and activate the *extrinsic* initiator caspases, caspase 8 and caspase 10. Processed caspase 8 subsequently activates the execution caspases caspase 3 and caspase 7. In peripheral mature T-lymphocytes, *extrinsic* caspase 8 driven apoptosis cannot be inhibited by transgenic overexpression of anti-apoptotic BCL-2 proteins[58].

1.1.3 Dysregulated T-cell apoptosis in human disease

Primary immunodeficiencies (PID) are genetically determined diseases of the immune system. PID may develop due to mutations of proteins involved in T-cell apoptosis, thereby causing a dysregulation of the immunological homeostasis[27,59–63]. Abnormal increase of apoptosis may cause immunodeficiency, whereas a failure of inducing RCD in immune cells can cause autoimmunity or non-malignant or malignant lymphoproliferation.

Loss of function mutations in the genes encoding for FAS or FASL cause autoimmune lymphoproliferative syndrome (ALPS). These patients suffer from non-malignant lymphoproliferation (lymphadenopathy, splenomegaly) and autoimmune cytopenia (autoimmune hemolytic anemia, immune thrombocytopenia, autoimmune neutropenia, often in combination). *In vitro* assessment of *extrinsic*, FAS-mediated apoptosis in T- cells of these patients reveals impaired apoptosis induction[64,65]. Mutations in the *SH2DA1* gene encoding for SAP have been identified to cause X-linked lymphoproliferative disease (XLP), another PID that leads to chronic non-malignant lymphoproliferation and a rather specific failure to control Epstein-Barr Virus (EBV). SAP deficiency seems to primarily affect T-cell RICD *via* complex mechanisms[66–68]. A clinically similar disease is observed in patients with loss of function mutations in XIAP. Besides lymphoproliferation and failure to control EBV, XIAP deficiency is frequently associated with severe and early onset inflammatory bowel disease. Also less rare, polygenic diseases are associated with dysregulated apoptosis and subsequent polyclonal lymphoproliferation. Such diseases include systemic autoimmune diseases such as rheumatoid arthritis (RA), sjögren's syndrome (SS) or systemic lupus erythematosus (SLE)[69–71]. Similarly, chronic virus infections such as infections with HIV or EBV are associated with lymphoproliferation caused by virus-mediated apoptotic evasion processes[61,72,73].

These clinical diseases exemplarily demonstrate that small molecule compounds that interfere with T-cell apoptosis processes have a high therapeutic potential in the treatment of immunological disorders.

1.2 Nur77, a nuclear orphan receptor

Many central cellular signaling pathways and key mediators have been investigated for their contribution to RCD. Important transcription factors that control RCD are NFκB[74] and p53[75] . The nuclear receptor superfamily contains at least over 60 nuclear transcription factors that regulate specific set of target genes[76]. Those, whose functional ligands have not been identified yet, are named nuclear orphan receptors[77]. A nuclear orphan receptor subfamily is the nuclear orphan retinoid receptor family NR4A (nuclear receptor subfamily 4, group A) with its members Nur77, Nurr1 and Nor1[78–80]. NR4A family members participate in important biological processes such as T-cell development[81,82], inflammatory responses[83], steroid hormone synthesis[84] and hepatic glucose metabolism[85]. Their association with cancer- and T-cell apoptosis is of particular interest[82,86,87].

1.2.1 Structure and functional domains of Nur77

Like most other nuclear receptors, the NR4A members share common functional structures such as a N-terminal region that contains a ligand-independent activation function-1 transactivation domain (AF-1TAD), a very conserved DNA binding domain (DBD), a hinge region and a ligand binding domain (LBD) in the C-terminus that contains a ligand-dependent AF-2TAD[77,88,89]. The N-terminal region functions as an adapter region to interact with other transcription factors[88]. The central DBD targets specific DNA structures, so called NGFI-B response- and Nur-responsive elements[90,91]. The LBD is in general responsible for binding small lipophilic molecules as ligands to induce specific cellular responses. Also, it contains heptad repeats of hydrophobic amino acids involved in nuclear receptor dimerization and may also be involved in targeting the right nuclear localization[88]. There seems to be a functional redundancy of Nur77 and other NR4A members, since the biochemical structure shows similarities. Some endogenous Nur77 ligands have been proposed in the recent years, such as stress signals and growth factors[80]. But most importantly, chemical compounds like Cytosporone-B (Csn-B, isolated from *Dothiorella sp. HTF3*, an endophytic fungus)[92,93] or synthesized derivates have been described as effective Nur77 ligands that induce Nur77-dependent cellular processes by binding to the Nur77 LBD[94–96].

1.2.2 Dual role of Nur77 in apoptosis

Due to its multifunctional binding sites, Nur77 acts as a connection mediator between different signaling pathways. With its ability to bind intracellular ligands, other transcription factors and its DNA binding motives, Nur77 shows optimal characteristics to regulate the cellular homeostatic balance.

A large number of studies implicate, that Nur77 induces apoptosis in various cancer cell lines with a high degree of complexity regarding the involved signal transduction[97,98]. Nur77 has been demonstrated to drive apoptosis in cultured cancer cell lines and in tumors *in vivo*, including melanomas[63,94,99–101], lymphomas[102,103], leukemia[104–107], lung cancer[108,109], prostatic cancer[109–112], breast cancer[107,113–115], ovarian cancer[116], colon cancer[117] and gastric cancer[114,118,119]. In some cancer types, Nur77 expression was even demonstrated to be predictive of poor prognosis, since reduced expression could be experimentally correlated to poorer overall survival[120].

Conversely, Nur77 has been identified to drive survival and support growth of certain cancer cell types[121–125]. Overall, these studies imply an essential and dual role of Nur77 in driving apoptosis *vs.* survival in cancer cells and tumors that depends on Nur77 cellular localization, expression[126] and accessability[127,128].

The signaling cascades, that are mainly involved by Nur77 associated apoptosis comprise *intrinsic*[30,129–131] and *extrinsic*[30,57] apoptosis. Nur77 driven *intrinsic* and *extrinsic* apoptosis pathways were mainly activated by MAPK (MEK, ERK1, ERK2, JNK and p38)[115,132–136] as well as the PI3K/AKT[87,137–140] signaling cascades.

Nur77 has been demonstrated to control expression of pro-apoptotic genes such as FASL or TRAIL[141,142]. In addition, Nur77, upon phosphorylation, has been shown to translocate from the nucleus to the cytoplasm where it interacts and inactivates anti-apoptotic Bcl-2 family members[143].

1.2.3 Role of Nur77 in T-cell apoptosis

In T-cells, Nur77 was originally described as an immediate-early induced gene[144] following *in vitro* activation of T-cells and subsequently as a gene induced by TCR engagement in T-cell hybridomas and thymocytes[82,145].

A dominant negative form of Nur77 impaired TCR-ligation mediated apoptosis (negative selection) upon overexpression in thymocytes[146–148].

Some studies reveal, that Nur77 phosphorylation impacts on its pro-apoptotic function, by inducing subcellular re-localization to the cytoplasm, specifically to the mitochondria [87,149,150]. Whether and how the translocation of Nur77 from the nucleus to the cytoplasm occurs in T-cells remains unclear. Transgenic overexpression of Bcl-2 in T-cells could not block Nur77

induced apoptosis[144]. The requirement of a correct TCR signaling with a proper co-stimulation or phorbol-ester stimulation for an immediate-early induction of Nur77 expression has been repeatedly demonstrated[86,151,152]. T-cells derived from immunodeficient patients with a genetically determined defect in calcium influx could not upregulate Nur77 following TCR stimulation compared to T-cells derived from healthy individuals[153].

Since the expression kinetics of Nor1 (*NR4A3*) following T-cell activation is comparable to Nur77 (*NR4A1*) and the structural homology of their LBD is approximately 90% (N- and C-terminus is divergent), a shared compensation and certain functional redundancy is very likely[154]. Functional redundancy between Nur77 and Nor-1 might also explain why a targeted gene knockout of *Nr4a1* (Nur77) did not show an obvious T-cell phenotype in mice[81,154]. The role of Nur77 in re-activation induced apoptosis of mature T-cells has to our knowledge not been experimentally addressed yet.

1.2.4 Modulating Nur77 driven apoptosis *via* small molecules

Nuclear receptors represent promising targets for medical compounds to treat cancer and metabolic diseases[97,155–158]. To date, no physiological ligand has been identified yet to bind the LBD of Nur77. A variety of small molecules have been used to induce Nur77-dependent apoptosis in different cell lines. These include 9-cis-retinoic acid and 1-di (3-indolyl)-1-(4-X-phenyl) methane[92,121], etoposide[159], 5,8 diacetoxyl-6-(1-acetoxy-4-methyl-3-pentenyl)-1,4-naphthaquinones[160] and 12 O-tetradecanoylphorbol-13-acetate[111,161]. Many of these studies proposed apoptosis induction *via* ligand induced heterodimerization of Nur77 with other retinoid receptors like retinoid x receptor (RXR) and subsequent translocation to the mitochondria.

1.2.5 Direct Targeting of Nur77 LBD by small molecules

The oktaketide **cytosporone-B** (Csn-B), isolated from *Dothiorella sp. HTF3*, an endophytic fungus, has been identified as a direct agonist of Nur77, binding to the Nur77 LBD and driving apoptosis by augmentation of the Nur77 transcriptional activity[93]. This resulted in reduced growth of gastric tumors and increased gluconeogenesis in the liver[109]. These cytosporone-B induced phenotypes were shown to depend on Nur77 expression as they were absent in *Nr4a1* (Nur77) knockout mice[93]. Apparently, Nor-1 (*Nr4a3*) was either not expressed or could not compensate for Nur77 in this model. More recent studies examined cytosporone-B derivate molecules, that contain the biochemical backbone of cytosporone-B, but were modified in specific residues to achieve more selective effects regarding apoptosis induction or glucose metabolism[94–96,162,163]. These studies revealed, that a Nur77 binding synthetic small molecule compound requires a benzene ring, the phenolic hydroxyl group and the acyl-chain, whereas the most important key feature regarding affinity and avidity

appeared to be the ester group[162]. The most interesting examples of the described small molecule compounds were ethyl 2-[2,3,4-trimethoxy-6-(1-octanoyl)phenyl]acetate (**TMPA**) and 1-(3,4,5-trihydroxyphenyl)nonan-1-one (**THPN**), depicted in **Figure 1**. TMPA was shown to lower blood glucose levels as efficient as metformin in overweight (type II diabetes-prone) mice *via* abrogating the binding of Nur77 to LKB1 in the nucleus, thereby blocking the activation of AMPKa in hepatocytes[96]. THPN led to efficient induction of *intrinsic* apoptosis selectively in melanoma cell lines and reduced melanoma growth *in vivo via* inducing Nur77 translocation to the mitochondrial outer membrane protein Nix[94,95]. Both compounds achieved their specific efficacy through a library-based change of the acyl group length compared to their parental compound cytosporone-B. Both, the TMPA and THPN –mediated effects were dependent on Nur77 and could not be compensated by other NR4A gene family members.

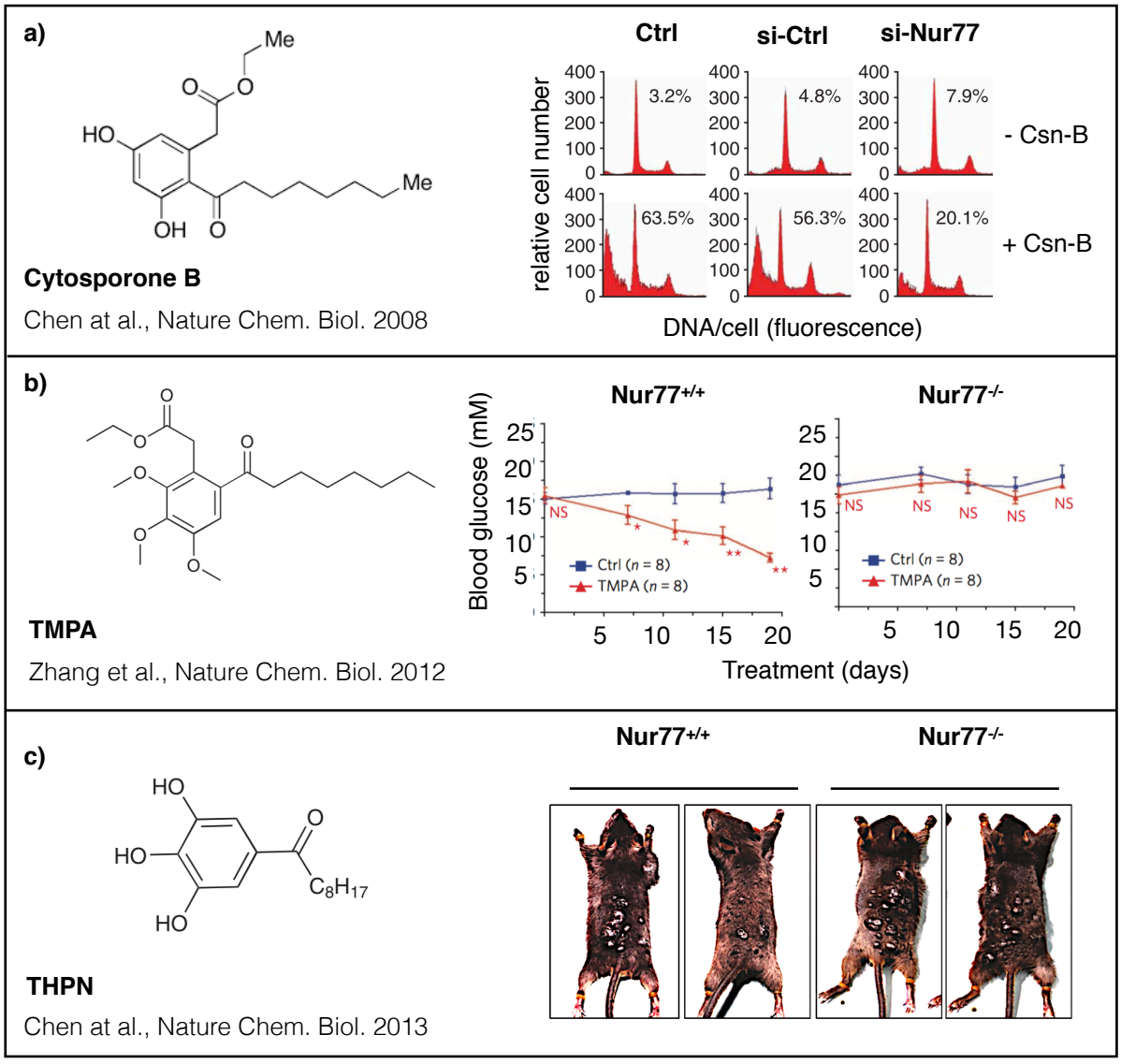

Figure 1 Nur77 binding small molecule compounds cytosporone-B, TMPA and THPN
a) Cytosporone-B (Csn-B, isolated from *Dothiorella sp. HTF3*, an endophytic fungus) has been identified as a direct agonist of Nur77 by binding to the Nur77 LBD resulting in apoptosis induction by augmentation of Nur77 transcriptional activity[93]. This resulted in reduced growth of gastric tumors and

increased gluconeogenesis in the liver[109]. **b)** TMPA (ethyl 2-[2,3,4-trimethoxy-6-(1-octanoyl)phenyl]acetate) has been demonstrated to lower blood glucose levels as efficient as metformin in overweight (type II diabetes prone) mice *via* abrogating the binding of Nur77 to LKB1 in the nucleus, thereby blocking the activation of AMPKa in hepatocytes. This effect was not present in Nur77$^{-/-}$ mice[96]. **c)** THPN (1-(3,4,5-trihydroxyphenyl)nonan-1-one) has been demonstrated to efficiently induce *intrinsic* apoptosis selectively in melanoma cells *via* inducing translocation of Nur77 to the mitochondrial outer membrane protein Nix[94,95]. THPN treatment led to enhanced remission of B16 melanomas *in vivo*. Again, this effect was not observed in Nur77$^{-/-}$ mice[94,95].

1.3 Potential of Nur77 binding small molecules to alter RICD in mature T-cells

The majority of small molecule compound-based Nur77 research concentrated on promoting Nur77 function to result in cancer control or in correcting metabolic dysregulations. The unique biological function of Nur77 in humans, including the role of Nur77 in the human immune system, remains unknown, as no single patient with a loss of function/loss of expression mutation in Nur77 has been described yet. Notably, the potential of targeting the Nur77 associated RICD using Nur77 binding small molecule compounds in mature T-cells remains largely unassessed.

The goal of my PhD thesis was to study the effect of previously described Nur77 binding small molecules on RICD in mature murine and human T-cells.

2 Material and Methods

Methods were all performed under optimized conditions according to established standardized operation protocols (SOP) in the lab.

2.1 Cell culture

2.1.1 Cell maintenance

Cell culture was performed under sterile conditions in a laminar flow hood (Thermo Fisher). Cells and cell lines were maintained at 37°C in a standard 5% CO_2 / 18% O_2 atmosphere in culture incubators (Hera cell). Cells were all maintained with supplemented complete RPMI medium (Sigma-Aldrich) containing Penicillin-Streptomycin (Pen-Strep, Gibco), non-essential amino acids solution (NEAA, Gibco), additional glutamine (Glutamax, Gibco) and 10% fetal calf serum (FCS, Gibco).

2.1.1.1 Freezing of cultured cells

For long-time storage, cells were washed with ice cold medium and then re-suspended in freezing solution consisting of fetal calf serum (FCS, Gibco) containing 10% dimethylsulfoxide (DMSO, Sigma-Aldrich) at a cell density of 5-10 x 10^6 cells/ml. Cells were transferred into specialized freezing tubes (Sarstedt) and tubes were placed at -80°C for 24 hours in a box, that is embedded in an isopropanol surrounded shell to preclude premature freezing. 24 hours later, freezing tubes were transferred into a liquid nitrogen tank to be stored for later experiments.

Human primary T-cells were isolated and maintained from fresh blood samples of blood donors from the local blood donor center of the University Hospital Basel following informed consent. Cells were either isolated from whole buffy coats derived from 500 ml blood donations (pre-processed to enrich the leucocyte part by centrifugation) or from two or three EDTA tubes containing 7.5ml peripheral blood.

2.1.2 Generation of splenocyte-derived murine primary T-cell blasts

To generate murine primary T-cell blasts, 327^{tg} mice, containing T-cells expressing a transgenic T-cell receptor-specific for the immunodominant MHC I restricted epitope (gp33-41) of lymphocytic choriomeningitis virus (LCMV)[164] were euthanized and spleens were removed. Splenocyte suspensions were created by careful application of pressure with a piston of a 5ml syringe and rinsing phosphate buffered saline (PBS) containing 2% FCS through 50μm pore size cell strainers (Corning). Subsequent incubation in hyperosmotic ACK lysis buffer (Qiagen) was performed to lyse erythrocytes. For expansion of LCMV-

specific T-cells, 2 x 10^6 splenocytes/ml were stimulated with LCMV derived gp33-41 peptide (1nM *in vitro*, IBA Life Science, Germany) plus recombinant IL-2 (300IU/ml, Proleukin®, Novartis,) in 25cm^2 culture flasks (Axonlab). T-cell blasts were expanded 1:1 every 2-3 days with fresh medium containing IL-2.

2.1.3 Isolation of human peripheral blood mononuclear cells (PBMC)

Peripheral blood mononuclear cells (PBMC) were directly isolated and maintained from fresh blood samples of blood donors from the local blood donor center of the University Hospital Basel following informed consent. EDTA blood- or buffy coat-derived PBMC were density-separated by loading EDTA blood onto the lymphoprep density gradient medium (Axis Shield) and centrifuged for 20 min at 400g with centrifuge deceleration efficacy set to 20%. After centrifugation, PBMC appeared as a white colored ring above the lymphoprep reagent. After transfer of PBMC into a 50ml Falcon tube and washing in PBS, erythrocyte lysis was performed by resuspension in one ml of hyperosmotic ACK erythrocyte lysis buffer (Qiagen) for five minutes. Subsequent washing with PBS was performed to dilute the lysis buffer and to remove leftovers of erythrocytes and cell debris. PBMC were then counted using a cell counter machine (NanoEnTek) and were then used directly for experiments or used to generate human primary T-cell blasts.

2.1.4 Generation of PBMC-derived human primary T-cell blasts

To study T-cell apoptosis and RICD in particular, primary human T-cell blasts were generated for re-stimulation experiments. PBMC were seeded into 96-well round bottom plates (Starlabs) with a cell density of 2-3 x 10^6 cells/ml in complete medium. PBMC derived T-cells were activated by adding 5 μg/ml phytohemagglutinin (PHA, isolated from the plant *Phaseolus Vulgaris,* Sigma Aldrich). In addition, human IL-2 (300IU/ml, Proleukin®, Novartis) was added to the medium. Every 4-7 days, cells were expanded 1:1 by adding the same volume of fresh complete medium containing fresh IL-2. After 2-3 rounds of expansion, primary T-cell blasts were used for re-stimulation experiments. Flow-cytometric analysis showed that primary T-cell blasts consisted of > 95% $CD3^+$ T-cells. While the $CD4^+/CD8^+$ T-cell ratio was normally >1 in PBMC-derived T-cells, the $CD4^+/CD8^+$ ratio was typically <1 in primary T-cell blasts (data not shown).

2.2 Cell biological methods

2.2.1 *In vitro* re-stimulation of primary T-cell blasts

To measure re-stimulation cell death (RICD) in primary T-cell blasts, cells were enriched for live cells by performing a ficoll-based separation or alternatively by using a bead-based negative selection (dead cell removal kit, Miltenyi) according to the manufacturer's protocol. Cells were seeded at a cell density of 2,5 x 10^6 cells/ml medium into 96-well U bottom plates (200µl final volume). T-cell re-stimulating stimuli or reagents were added as outlined below (**Table 1**). Nur77 binding small molecule compounds (cytosporone B, TMPA or THPN) were added directly before applying the stimuli at the indicated concentrations. Specific inhibitors of signaling were added 30 minutes before re-stimulation (if not further specified). The standard incubation time before assessing RICD was four hours.

Table 1 Stimuli or reagents used for re-stimulation bioassays

Reagent or antibody (clone)	[c] final	Company
PMA (Phorbol ester)	5ng/ml	Sigma-Aldrich
PHA (Phytohemagglutinin)	0,5 – 5 µg/ml	Sigma-Aldrich
Staurosporine (Indolcarbazole)	0,5 - 2 µM	Sigma-Aldrich
Anti CD28 (CD28.2)	0,5 – 5 µg/ml	Biolegend
Anti CD3 (OKT3)	0,5 – 5 µg/ml	Biolegend
Anti FAS (EOS9.1)	0,5 – 5 µg/ml	Biolegend
Recombinant FASL	50 – 500 ng/ml	ebioscience
gp33-41 peptide	1 - 10 nM	Iba lifesciences
OVA peptide	1 – 10 pM	Anaspec Inc.
Cytosporone-B	1 – 100 µM	Sigma
TMPA	1 – 100 µM	Merck
THPN	0.5 – 50 µM	Merca Chem
U0126	1 µM	Sigma
PD184352	10 µM	Sigma

2.2.2 Transfection of cells with siRNA

To investigate the causative role of a single gene and its encoded protein on T-cell RICD, genes of interest were knocked down by targeting them with small interfering RNA (siRNA). These siRNAs were transfected into the cells by electroporation using the AMAXA device (Lonza). T-cell blasts were prepared for transfection in specialized glass cuvettes (Lonza) by

washing and subsequent resuspension in transfection solution (transfection kit for activated T-cells or cell lines, Lonza). The specific siRNA and a non-specific control siRNA (mix of several unspecific sequences, Qiagen) was diluted with transfection solution at the concentration specified in **Table 2**. Specific siRNA were used in combination with total concentration of 100nM. T-cell blasts were afterwards re-suspended with fresh medium and rested for 24 hours before they were used for experiments.

Table 2 siRNA used for transfection

siRNA target	siRNA	[c] final	Company
Nur77 (*NR4A1*)	Flexitube siRNA (2)	25nM	Qiagen
Nur77 (*NR4A1*)	Flexitube siRNA (3)	25nM	Qiagen
Nur77 (*NR4A1*)	Flexitube siRNA (5)	25nM	Qiagen
Nur77 (*NR4A1*)	Flexitube siRNA (6)	25nM	Qiagen
Nor1 (*NR4A3*)	Gen Solution siRNA (2)	25nM	Qiagen
Nor1 (*NR4A3*)	Gen Solution siRNA (4)	25nM	Qiagen
Nor1 (*NR4A3*)	Gen Solution siRNA (5)	25nM	Qiagen
Nor1 (*NR4A3*)	Gen Solution siRNA (6)	25nM	Qiagen
Control siRNA	AllStars negative control	100nM	Qiagen

2.3 Flow Cytometry

Flow-cytometry was performed to assess T-cell proliferation and T-cell apoptosis in specific T-cell subpopulations. Flow cytometric analysis was performed with the flow-cytometers Accuri (BD bioscience), Cytoflex (Beckman Coulter) or Fortessa (BD bioscience).

2.3.1 Flow-cytometric phenotyping based on surface protein expression

For flow-cytometric phenotyping of freshly isolated PBMC derived T-cells, cells were seeded at a density of 2-3 x 10^6 cells/ml and washed two times with PBS/1% FCS (FACS buffer). Washed cells were re-suspended in 100 μl of FACS buffer containing a mixture of fluorescent staining antibodies at a dilution of 1:100 (if not further specified). Incubation with the staining antibody solution was 30 minutes at room temperature (RT) or at four degrees. Most staining antibodies were directly conjugated with a fluorochrome. For staining with non-conjugated antibodies, a two-step staining was performed. Here, a fluorochrome-labeled secondary antibody against the immunoglobulin isotype of the non-labeled primary antibody

was used to generate a fluorescence signal for the flow-cytometric analysis. Non-specific isotype antibodies were used to define the background fluorescence signal.

To correct for overlaps of the fluorochrome emission spectra, that could not be avoided by a mathematical compensation, a single stain sample of every used fluorochrome was prepared for every flow-cytometric analysis that used more than two lasers. A list of antibodies used for flow-cytometric analysis is given in **Table 3**.

Table 3 Antibodies used for staining of surface proteins

Epitope human (clone)	[c] final	Fluorochrome	Company
Primary antibodies			
CD3 (UCHT1)	0.5 µg/ml	PE, APC, Alexa700	Biolegend
CD8 (SK1)	0.5 µg/ml	Alexa488, PE-Cy7	Biolegend
CD4 (SK3)	0.5 µg/ml	PE, PE-Cy7	Biolegend
Epitope murine (clone)	**[c] final**	**Fluorochrome**	**Company**
Primary antibodies			
CD3 (17A2)	0.2 µg/ml	PE	ebioscience
CD8 (53-6.7)	0.2 µg/ml	Pacific Blue	ebioscience

2.3.2 Phenotyping of splenocyte-derived murine LCMV-specific transgenic primary T-cells and T-cell blasts

Expression of the transgenic TCR-α (Vα2) and TCR-β (Vβ8.1), derived from a T-cell line specific for the immunodominant MHC I restricted epitope gp33-41 of lymphocytic choriomeningitis virus (LCMV)[165,166], in 327^{tg} mice was verified by flow-cytometric analysis. Murine splenocytes were stained with fluorochrome-labeled monoclonal antibodies specific for TCR Vα2 and Vβ8.1 (**Table 4**) according to 2.3.1.

Table 4 Antibodies used for flow-cytometric phenotyping of 327^{tg} mice

Epitope murine (clone)	[c] final	Fluorochrome	Company
Primary antibodies			
Vα2 TCR	2,5 µg/ml	FITC	BD Pharmingen
Vβ8.1 TCR	2,5 µg/ml	Alexa647	Biolegend

2.3.3 Assessing apoptosis by flow-cytometry using annexinV binding

Apoptotic cells, in contrast to live cells, are characterized by phosphatidylserine (PS) expression at the outer cell membrane[167]. At high calcium concentrations, annexinV binds specifically to phosphatidylserine. Therefore, fluorochrome-coupled annexinV can be used to identify apoptotic cells by flow-cytometry. To assess T-cell apoptosis by flow-cytometry, T-cell blasts were washed two times with annexinV binding buffer (Biolegend) and subsequently stained with fluorochrome-labeled annexinV diluted 1:100 in annexinV binding buffer for 30 minutes at RT.

Additionally, 7-Aminoactinomycin (7-AAD) was used to distinguish early apoptotic cells (annexinV$^+$) from late apoptotic or necrotic cells (annexinV$^+$ 7-AAD$^+$) (**Table 5,** data not shown). Co-staining with antibodies specific for cell surface proteins was performed in the same buffer (according to 2.3.1).

Table 5 Reagents used for cytometry-based assessment of apoptotic cells

Reagent	[c] final	Fluorochrome	Company
annexinV	1 μg/ml	FITC, PE, APC	Biolegend
7-AAD	0.5 μg/ml	autofluorescent	ebioscience

2.3.4 Flow-cytometric analysis of intracellular, nuclear and phosphorylated proteins

RICD associated changes in protein biosynthesis were assessed by flow-cytometric analysis. T-cell blasts were fixed using fixation buffer (Fix/Perm, BD bioscience) according to the manufacturer's protocol (BD bioscience). Saponin based buffers (BD Perm/wash) are milder than methanol based buffers (BD Perm III), the latter leading to linearization of proteins which deteriorates binding of many flow-cytometry antibodies due to destruction of the secondary and tertiary protein structures. Linearization of proteins is however required to measure phosphorylation of proteins by flow-cytometry. Methanol based buffers (Perm III, BD bioscience) but also saponin based buffers (Perm/wash, BD bioscience) permeabilize the nuclear membrane. Therefore, methanol- or saponin based buffers were used to flow-cytometrically quantify intranuclear proteins while flow-cytometric assessment of protein phosphorylation required the use of methanol based buffers.

Following fixation and permeabilization, T-cell blasts were stained with fluorochrome conjugated antibodies in the required buffer for 30-45 minutes at RT. For non-conjugated

antibodies, secondary fluorochrome-labeled antibodies were used. **Table 6** summarizes the utilized antibodies.

Table 6 Antibodies used for intracellular-, nuclear- and phospho-protein staining

Epitope human (clone)	[c] final	Fluorochrome	Company
Primary antibodies			
Nur77 (D63C5)	0.7 µg/ml	-	Cell Signaling
p-Nur77 Ser351 (D22G5)	0.6 µg/ml	-	Cell Signaling
Rabbit mAb IgG Isotype Ctrl (DA1E)	Adjusted to experiment	-	Cell Signaling
SAP (1C9)	4 µg/ml	-	Abnova
IgG 1 κ Isotype Ctrl	4 µg/ml	-	Abnova
IFNγ (B27)	2 µg/ml	PE	biolegend
TNFα (MAb11)	1 µg/ml	PE	ebioscience
Secondary antibodies			
Fab_2 fragment goat anti rabbit IgG	0.75 µg/ml	Alexa647	Jackson Immunoresearch
Epitope murine (clone)	**[c] final**	**Fluorochrome**	**Company**
Primary antibodies			
IFNγ (MOB-47)	4 µg/ml	PE	Biolegend
TNFα (MP6-XT22)	2 µg/ml	FITC	Biolegend
Nur77 (12.14)	1 µg/ml	PE	ebioscience
Mouse IgG 1 κ Isotype Ctrl	1 µg/ml	PE	ebioscience

2.3.5 Assessing primary T-cell proliferation by flow-cytometry using CFSE

To measure T-cell proliferation kinetics *in vitro*, cells were labeled with Carboxyfluorescein succinimidyl ester (CFSE), a fluorescent cell staining dye, that covalently couples to intracellular proteins containing lysine or other amine residues. Due to its covalent coupling, the dye retains in the cell and is diluted with every cell division. Thus, loss of fluorescence is directly correlated with cell proliferation. To assess cell proliferation in primary T-cells, 3 x 10^6 PBMC/ml were washed two times with PBS and subsequently stained with CFSE containing PBS (5 µM, Thermo Fisher) for ten minutes at 37°C. Unbound dye was removed by washing the cells twice in ice cold complete medium. Cells were then stimulated with anti-CD3/CD28 antibodies (5 µg/ml each, Biolegend) or PHA (5 µg/ml, Sigma Aldrich) to activate T-cells. In

addition, IL-2 (300IU/ml, Proleukin®, Novartis) was added to the medium. For assessment of T-cell proliferation, CFSE fluorescence of $CD3^+$ T-cells was analyzed by flow-cytometry.

2.3.6 Assessing mitochondrial membrane potential by flow-cytometry using TMRE

Intrinsic apoptosis pathways as described above involves mitochondrial damage by MOMP. This membrane potential drop during permeabilization can be measured by incubating cells with a fluorescent dye (TMRE), that accumulates in intact mitochondria due to its positive charge. Depolarized or disrupted mitochondria cannot anymore sequester TMRE within mitochondria. Therefore, TMRE can be used to flow-cytometrically assess the drop of the mitochondrial membrane potential in apoptotic cells. Four hours after T-cell RICD induction, T-cell blasts were cultured for additional 30 minutes in medium containing 100 nM TMRE according to the manufacturer's protocol (Immunochemistry Technologies). Following washing, T-cell blast-*intrinsic* TMRE fluorescence was measured by flow-cytometry as described in 2.3.1.

2.3.7 Assessing caspase activation by flow-cytometry using FLICA®

Intrinsic and *extrinsic* apoptosis involves proteolytic cleavage of effector caspases leading to caspase activation Caspase activation can be measured by incubating re-stimulated T-cells with the fluorochrome-labeled specific caspase inhibitors (FLICA) FAM-LEHD-FMK (caspase 9-specific) or FAM-LETD-FMK (caspase 8-specific). The cell-permeable, fluorescent reagents become covalently coupled to the activated caspases. Therefore, cellular fluorescence is directly linked to activation of caspases during T-cell RICD.

Four hours following induction of T-cell RICD, cells were incubated with medium containing 50 - 200 nM of the FLICA®-reagent for additional 30 minutes at 37°C according to the manufacturer's protocol (Immunochemistry Technologies). Subsequently, cells were stained and analyzed by flow-cytometry as described in 2.3.1.

2.4 Molecular biological methods

All molecular biological methods to analyse RNA and DNA were performed under non-sterile but clean and nuclease free conditions. Basis material for RNA or genomic DNA extraction were cell lysates ($1 – 5 \times 10^6$ cells) derived from frozen cell pellets or from fresh cell pellets, that were frozen after re-suspension in Trizol reagent (ambion, life technologies) at -20°C.

2.4.1 RNA extraction from cell lysates

For RNA extraction, cell lysates re-suspended in Trizol reagent were thawed and chloroform was added at 20% of total volume. RNA isolation was performed using an QIAamp RNA blood mini kit according to the manufacturer's instructions (Qiagen). Final elution volume was 25 – 50 μl in nuclease free water. RNA concentration was measured with a nanodrop machine (Thermo Fisher Scientific).

2.4.2 Reverse transcription

Prior to reverse transcription, RNA was first digested with a DNAse I Amplification Grade Kit (Sigma) at 37°C for 30 minutes in PCR tubes (Sarstedt). DNAse was subsequently inactivated for 10 minutes at 65°C. Then, annealing of random primers (Promega) was allowed at 70°C. A master mix with all essential reverse transcription reaction reagents was applied directly with the annealed RNA-Primer mix including a control condition with nuclease free water. Reverse transcription using the GoTaq G2 DNA Polymerase (Promega) was finally performed in a TProfessional TRIO PCR Thermocycler (Core Life Sciences) according to manufacturer's protocol (GoScript Reverse Transcription System). cDNA was stored at 4°C or directly used for analysis.

2.4.3 Quantitative real time PCR (qPCR)

cDNA was directly used for qPCR analysis. qPCR was performed using a Sybr Green® method (Promega). Specific primers for qPCR were designed with a free open source software *Primer Blast* of the NCBI databank. The *FASTA*-file from the NCBI gene card was used as a matrix to create specific oligos, that overlapped at least two exons and had a predicted product size of not more than 150 base pairs. Primer length was around 20 – 23 bases (**Table 8**). Primer oligos were synthesized by a company (Microsynth). In addition, mRNA levels of at least two reference genes were analyzed in parallel. Examples for reference genes were *GAPDH* and *ACTIN* (for unstimulated conditions) or *18S* and *IPO8* (for stimulated conditions). Finally, cDNA expression levels measured in re-stimulated T-cells were compared in relative units (fold change) to transcription levels under non-stimulated conditions. All samples were additionally normalized to the expression levels of the reference (housekeeping) genes. The PCR was prepared according to the manufacturer's protocol (Promega). A GoTaq qPCR Master Mix (Promega), containing all essential reaction reagents was used together with the sample cDNA (and a control condition with nuclease free water) and the specific primers (forward and reverse) in FAST qPCR® 96-well plates (R&D Systems). The plate was sealed with a foil to prevent evaporation and qPCR was performed in a qPCR cycler ABI machine (Applied biosystems, Thermo Fisher Scientific) (settings are

displayed in **Table 7**). A FAST qPCR with 40 cycles (two-hours runtime) and a melting curve was performed.

QPCR data were finally saved on a common lab server for later analysis. For data analysis, quantification equation based on a publication by W. Pfaffl was used[168].

Table 7 qPCR program settings

Temperature	Time	Cycles
50°C	2 min	1
95°C	10 min	1
95°C	15 sec	40
60°C	1 min	

Table 8 primer sequences used for qPCR

Gene	Forward	Reverse
Human		
NR4A1	GATCGGTCCCCAAAGGATG	TGAGGGTCTGGGCATAGAA
NR4A3	TGCAAAGCTGTCCATTACAC	GCATCCTCCACGAGCAAGT
SH2D1A	GGCAGCTATTTGCTAGGGA	TCTGTCTGGGAACTCGGTA
SH2D1B1	GACAGCGAGTCGATCCAGG	ACCCGTGTTTCCTCTGAAG
SLAMF1	GCTCCTCTCCTTGACTTCG	CCGGAGAATCTTGGGCAGT
SLAMF6	CTCTCGGACTGAGAACGCA	CGCAGGCTGAATTGTCTAC
Murine		
Nr4a1	AGTTGGGGGAGTGGCTAGA	GCTCGTTGTGGTGTTCCAT
Nr4a3	ACTGCATCTTGGTTTGCAG	TCTTCCAATCTATGCCACTTG
Sh2d1a	CGAGTGTCCCAGCAGAAAA	GGATACGCAGAGGCGTCAC

2.4.4 Genomic DNA extraction and endpoint PCR

For genotyping or DNA sequencing, genomic DNA was extracted from dried, frozen cell pellets or from mouse tissue (earpunch biopsies) according to the manufacturers protocol (Qiagen). For DNA extraction, a rapid protocol with a ready-to-use master mix was used (Kapa biosystems). DNA extraction was performed at 56°C on a shaker using the Kapa express extract buffer. Genomic DNA could subsequently be used for endpoint PCR or stored for later analysis at 4°C.

For endpoint PCR, the master mix with the specific primers to amplify the sequence of interest was added. Amplification was performed using the GoTaq G2 DNA Polymerase

(Promega). The PCR program (according to manufacturer's protocol, Promega) was performed in a TProfessional TRIO PCR Thermocycler (Core Life Sciences) (**Table 9**). Primers were designed according to 2.5.4 (**Table 6**). Primer sequences specific for detection of Nur77 knock-out mice were used as described in previous studies reporting these mice[160] (**Table 10**).

Table 9 endpoint PCR program settings

Temperature	Time	Cycles
95°C	2 min	1
95°C	20 sec	38
62°C	20 sec	
72°C	45 sec	
72°C	5 min	1

Table 10 Primer sequences used for Nur77 genotyping

Gene	Forward	Reverse
Murine		
Nr4a1	TCATGGACGGCTACACAG	GTAGGCATGGAATAGCTC

2.5 RNA Sequencing

RNA sequencing experiments were performed in RNA samples derived from re-stimulated T-cells derived from 327^{tg} mice, where most $CD8^+$ T-cells are specific for the immunodominant lymphocytic choriomeningitis virus (LCMV) peptide gp33-41[164–166]. LCMV-specific $CD8^+$ T-cell blasts were re-stimulated *in vitro* for four hours using the gp33-41 peptide (1nM) in the presence or absence of titrated amounts of TMPA. The use of transgenic T-cells allowed a standardized experimental setup in which differences due to genomic variance could be minimized.

2.5.1 Sample preparation and transcriptome analysis

Splenocytes from four different 327^{tg} mice were *in vitro* stimulated with the LCMV derived gp33-41 peptide in the presence of IL-2 (300IU/ml). 8 days later, expanded T-cell blasts were re-stimulated with gp33-41 peptide in the absence or presence of TMPA (5 and 50 µM). All four 327^{tg} mice were processed on four different days, including the expansion of splenocytes and the final re-stimulations assays.

For generation of RNA, 1,5 x 10^6 cells were lysed in a special lysis buffer for RNA extraction (Machery-Nagel). Lysis volume was 200 µl. The lysates were directly frozen at -80°C. RNA

extraction and the subsequent preparation for RNA sequencing, including the creation of an RNA library was outsourced to the sequencing facility at the Biocentre of Basel, headed by Phillipe Demougin. RNA sequencing was then performed at the core facility of the DBSSE Basel. The statistical evaluation and the implementation of the sequencing raw data into a specific analysis online tool was performed by Julien Roux, bioinformatics core facility of the Department of Biomedicine Basel. Detailed and structured comparison between unstimulated and stimulated conditions on the one hand, and untreated and treated conditions on the other hand, regarding significance and multiple component analysis, was performed with Microsoft Excel 2016, Prism7 and curated databases for pathway mapping analyzes based on *pathwayseq*[169].

3 Results

3.1 Nur77 is rapidly induced during primary human T-cell RICD preceding *intrinsic* apoptosis induction

Beside metabolism[85], insulin sensitivity[170], obesity[171] and onset and progression of various cancer types[156], a repeatedly demonstrated function of Nur77 was to promote apoptosis during thymocyte development and during T-cell RICD[82,86,151]. The exact role of Nur77 in re-stimulated mature human T-cells however has not yet been assessed yet.

3.1.1 Experimental assessment of RICD in primary human T-cell blasts

To assess the role of Nur77 in RICD in mature human T-cells, assays were established to measure apoptosis following re-stimulation of expanded primary human T-cell blasts (see methods). Apoptosis induction was monitored using different flow-cytometry based methods (representatively shown in **Figure 2**). These consisted of **a)** quantifying annexinV binding to exposed phosphatidylserine at the outer T-cell membrane, **b)** assessment of mitochondrial outer membrane potential by incubating re-stimulated T-cells with the fluorescent, mitochondria-affine and mitochondrial potential-sensitive compound TMRE and **c)** flow-cytometric assessment of fluorescently-labeled caspase 9 inhibitor (FLICA)-binding to activated caspase 9, the initiator caspase of the *intrinsic* apoptosis signaling pathway. In the absence of re-stimulation, primary $CD3^+$ human T-cell blasts displayed as two prominent cell populations based on forward- (FSC) and side scatter (SSC) flow-cytometric analysis. These populations represent 'live' (high FSC) *vs.* 'dead' (low FSC) T-cell populations based on apoptosis marker expression (**Figure 2**). Already four hours after re-stimulation of primary T-cell blasts with the phorbol ester PMA (Phorbol-12-myristat-13-acetat), the 'live' population was relatively reduced and a relative increase of the 'dead' T-cell population was observed. Within the 'live' gate, PMA induced apoptotic changes on a subfraction of T-cell blasts, while almost all cells within the 'dead' gate expressed an apoptotic phenotype (**Figure 2**). Based on these results, all subsequent measurements of T-cell apoptosis are based on flow-cytometric analysis of T-cells within the 'live' gate.

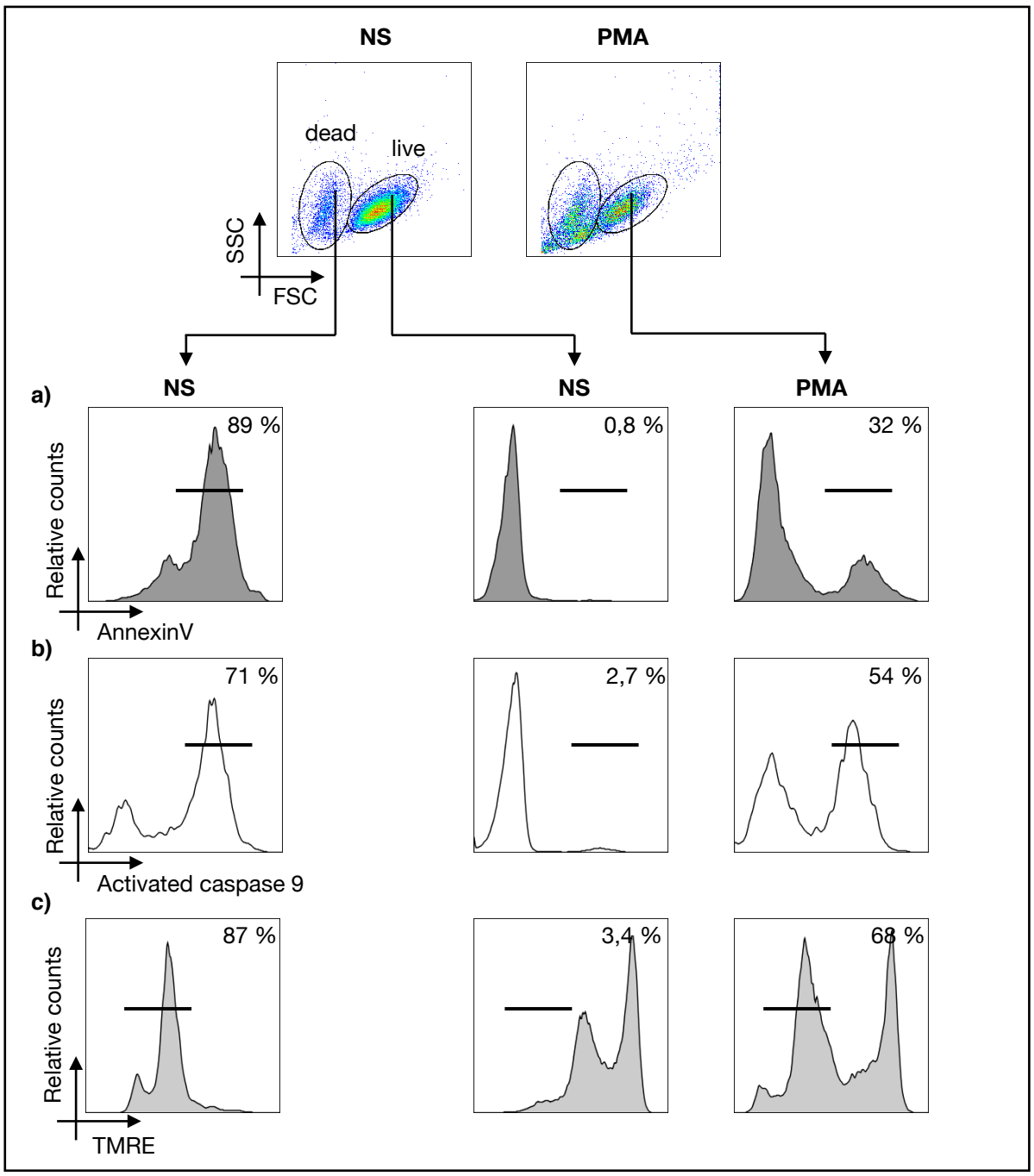

Figure 2 Flow-cytometric assessment of apoptosis in primary human T-cell blasts
Primary human T-cell blasts were re-stimulated with PMA or left non-stimulated for four hours in medium. Cells were gated on $CD3^+/CD8^+$ expression for flow-cytometric analysis of $CD8^+$ T-cell apoptosis. Forward- (FSC) *vs.* side scatter (SSC) analysis revealed two populations of T-cells, which could be attributed to 'live' *vs.* 'dead' cell fractions based on the cell size and expression of markers of apoptosis (see below). Apoptotic cells were defined as $annexinV^+$, activated Caspase 9^+ and $TMRE^{lo}$. **a)** PMA re-stimulation induced a subfraction of apoptotic, $annexinV^+$ $CD8^+$ T-cells within the 'live' gate. Within the 'dead' gate, almost all cells were $annexinV^+$. **b)** For assessment of caspase 9 activity, T-cell blasts were incubated with the fluorochrome-labeled caspase 9-specific inhibitor FAM-LEHD-FMK (100 nM) for the last 30 minutes of culture according to the manufacturer's protocol (Immunochemistry technologies) and subsequently stained for CD3 and CD8 prior to flow-cytometric analysis. Following PMA stimulation, a subfraction of T-cell blasts displayed activated caspase 9 (see representative histograms). **c)** For assessment of T-cell blast *intrinsic* mitochondrial potential, T-cells were incubated at 37°C for the last 30 minutes of culture in medium containing TMRE (100nM) according to the manufacturer's protocol (Immunochemistry technologies) and subsequently stained for CD3 and CD8 before analysis by flow-cytometry. PMA re-stimulation for four hours was associated with increased frequencies of $TMRE^{lo}$ T-cell blasts, indicative for loss of mitochondrial outer membrane potential.

3.1.2 Nur77 induction and phosphorylation in re-stimulated primary human T-cell blasts

Nur77 has been reported to exert its functions depending on tissue context, in which it is expressed and on the subcellular expression compartment[119]. Whereas Nur77 is constitutively expressed in cancer cell lines[155], its expression in T-cells requires signaling *via* the T-cell receptor[82]. To assess Nur77 and its role in T-cell RICD, we monitored Nur77 expression by flow-cytometry early after re-stimulation. (**Figure 3**).

Primary human T-cell blasts were re-stimulated *in vitro* with PMA to induce *intrinsic* apoptosis. *In vitro* incubation with an agonistic anti-FAS antibody induced *extrinsic* apoptosis as control. In a representative experiment, both conditions induced considerable T-cell apoptosis within four hours (PMA 61% annexinV$^+$ *vs.* aFAS 49% annexinV$^+$). However, Nur77 expression was only detected in cells re-stimulated with PMA (55% Nur77$^+$), while aFAS treatment induced apoptosis in the absence of Nur77 expression (**Figure 3a**). The results observed following aFAS *in vitro* treatment also suggested that T-cell *intrinsic* Nur77 expression is not a *per se* consequence of T-cell apoptosis (**Figure 3a**).

To test, which major kinase cascade regulates early Nur77 induction following PMA re-stimulation, two inhibitors for the mitogen activated protein kinases (MAPK) MEK/ERK pathway (U0126[172] and PD184352[173]) were incubated with primary human T-cell blasts prior to induction of RICD . Both inhibitors almost completely blocked Nur77 induction two hours following PMA re-stimulation in primary human T-cells (**Figure 3b**).

In keeping, activation of caspase 9 following PMA induced T-cell re-stimulation was reduced in the presence of these two inhibitors (**Figure 3c**).

Thus, Nur77 was rapidly induced following MEK/ERK signaling in re-stimulated primary human T-cell blasts, correlating with apoptosis induction *via* the *intrinsic* apoptosis pathway.

Next, we experimentally tested whether direct targeting of Nur77 with a Nur77 LBD binding small molecule compound (TMPA[96]) influenced Nur77 expression and Nur77 phosphorylation in re-stimulated human T-cell blasts. Nur77 phosphorylation has been reported to drive Bcl-2-dependent apoptosis in cancer cells[143]. Treatment of primary human T-cell blasts with TMPA (low and high dose (10μM + 50μM)) during re-stimulation did not impact on Nur77 expression as analyzed by flow-cytometry, neither in PMA re-stimulated cells, nor in cells re-stimulated by TCR crosslinking with an agonistic anti-CD3 antibody (aCD3, clone OKT3) (**Figure 3d**). TCR crosslinking by agonistic aCD3 antibody led to impaired Nur77 protein induction compared to PMA re-stimulation (**Figure 3d**). FAS crosslinking did not induce Nur77 expression, neither in the presence nor in the absence of TMPA (**Figure 3d**). Nur77 phosphorylation was also assessed by flow-cytometry using an antibody detecting the phosphorylation of a Serine at position 351. Similar to total Nur77

protein expression, Nur77 phosphorylation was augmented in PMA re-stimulated T-cell blasts compared to TCR crosslinking, while no phosphorylation could be detected as a consequence of FAS crosslinking (**Figure 3d**). Treatment with low dose TMPA (10μM) did not impact on Nur77 phosphorylation, whereas high dose TMPA reduced RICD associated Nur77 phosphorylation, both following PMA or aCD3 re-stimulation (**Figure 3d**). In summary, the Nur77 binding small molecule compound TMPA did not alter Nur77 induction during T-cell RICD, while reduction of Ser351 phosphorylation was dose-dependent..

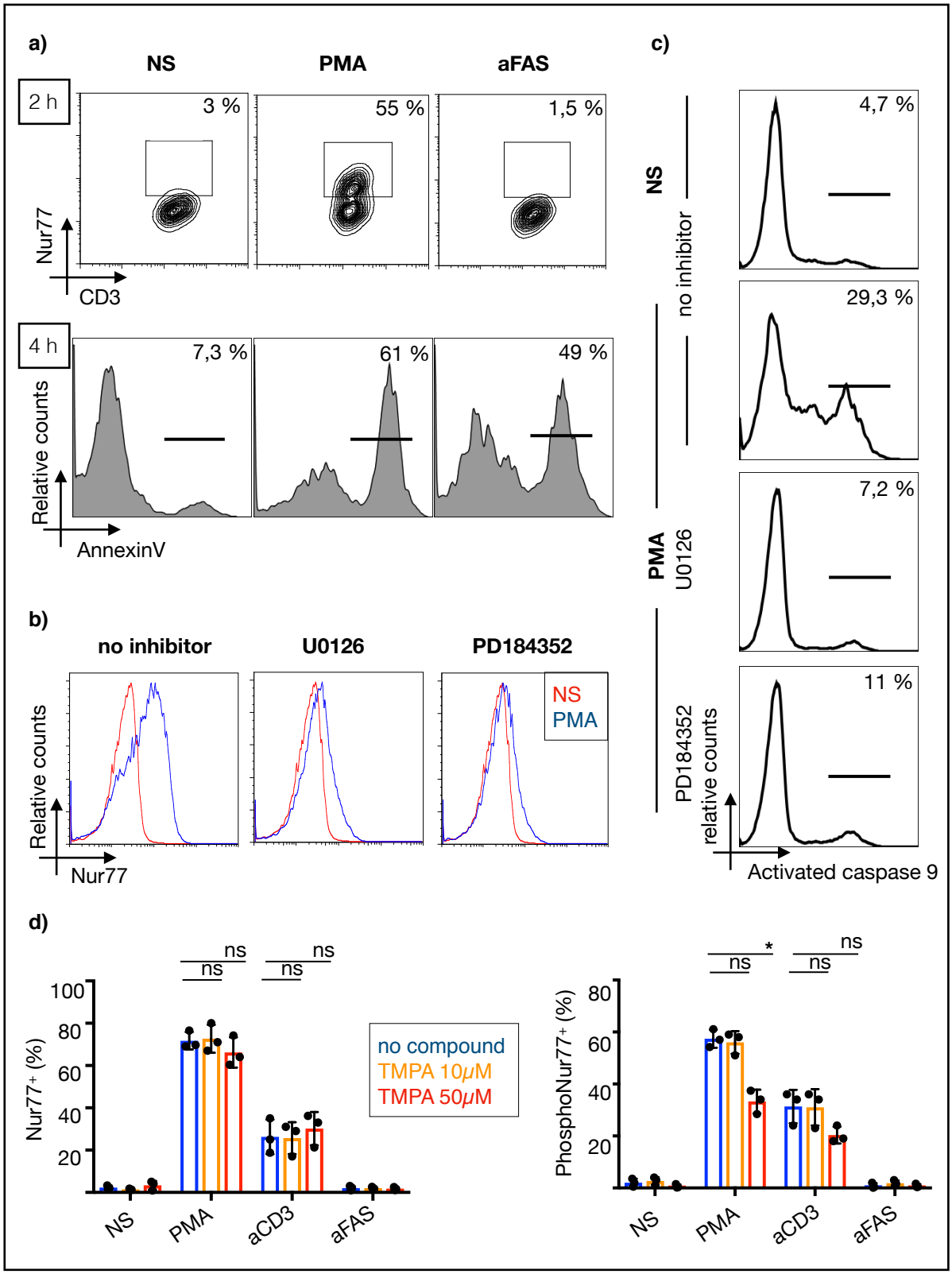

Figure 3 Nur77 induction following MEK/ERK driven T-cell activation

a) Primary human T-cell blasts were re-stimulated with PMA, treated with agonistic FAS-specific monoclonal antibody (aFAS) or left unstimulated for two hours in RPMI medium. T-cell blasts were subsequently assessed for Nur77 expression with a two-step staining protocol and flow-cytometric analysis according to 2.3.4. For assessment of T-cell RICD, T-cell blasts were re-stimulated with PMA, treated with agonistic aFAS antibody or left unstimulated for four hours and subsequently stained with annexinV and analyzed by flow-cytometry according to 2.3.3. Results from representative experiments are shown. **b)** Primary human T-cell blasts were incubated with the MEK inhibitors U0126 (1 μM) and PD184352 (10 μM) for 30 minutes prior to re-stimulation with PMA. Nur77 expression was analyzed by

flow-cytometry two hours after re-stimulation. **c)** Caspase 9 activation was assessed by flow-cytometry four hours after PMA re-stimulation according to 2.3.6. Primary human T-cell blasts were incubated with the MEK inhibitors U0126 (1 μM) and PD184352 (10 μM) for 30 minutes prior to re-stimulation as indicated. Representative histogram plots are shown. **d)** To assess Nur77 expression and Nur77 phosphorylation, primary human T-cell blasts were re-stimulated with PMA, agonistic anti-CD3 monoclonal antibody (aCD3, clone OKT3), treated with agonistic FAS-specific monoclonal antibody (aFAS) or left unstimulated in medium. The Nur77 binding small molecule compound TMPA was added at indicated concentrations prior to T-cell stimulation. Two hours later, expression of Nur77 or phospho-Nur77 (Ser351) was assessed using specific monoclonal antibody staining followed by flow-cytometric analysis according to 2.3.4. The summary graph shows mean and standard deviation of experiments performed using T-cell blasts derived from N=3 healthy donors.
Cells were gated on $CD3^+/CD8^+$ expression for flow-cytometric analysis. Statistics were performed using a two-way-ANOVA test; ns indicates non-significant changes, * = p<0,05, ** = p<0,01, *** = p<0,001.

3.2 Assessment of human T-cell RICD in the presence of Nur77 binding small molecule compounds

To date, no endogenous ligand has been described for Nur77. Several studies have investigated the pro-apoptotic role of Nur77 by targeting the Nur77-LBD with small molecule compounds to modulate its function[93,95,96,162]. All of these studies have analyzed apoptosis induction in cancer cell lines. Direct targeting of Nur77 in primary murine and human T-cells has not been addressed yet. To test, whether previously described small molecule compounds impact on RICD in primary human T-cells, apoptosis was monitored following re-stimulation in the presence *vs.* absence of Nur77 targeting small molecule compounds (**Figure 4**).

3.2.1 TMPA and THPN impair human T-cell RICD

Primary human T-cell blasts were *in vitro* re-stimulated with PMA and apoptosis was monitored by annexinV staining and flow-cytometry four hours later. Non-re-stimulated cells served as a control (**Figure 4**). Cytosporone-B, TMPA and THPN were titrated into T-cell blast cultures at different concentrations before re-stimulation to generate *in vitro* dose-response curves of each compound. Cytosporone-B and THPN induced re-stimulation-independent T-cell death at concentrations above 50μM (**Figure 4a**). In contrast, TMPA did not induce spontaneous T-cell death even at high concentrations. At high doses, cytosporone-B reduced T-cell RICD, however, since these concentrations also induced non-re-stimulation induced apoptosis, the significance of this finding remained unclear (**Figure 4a**). TMPA significantly reduced T-cell RICD in a dose-dependent manner, starting at 10μM. THPN also significantly reduced T-cell RICD at concentrations of 1 and 10μM. Higher concentrations of THPN, similar to cytosporone-B, induced non-re-stimulation associated T-cell apoptosis (**Figure 4a**).

TMPA and THPN were further analyzed for their ability to reduce T-cell RICD in N=8 healthy donors to proof consistency of efficacy. Both, TMPA and THPN demonstrated consistent, dose-dependent reduction of T-cell RICD (**Figure 4b**).

Since TMPA did not display any cytotoxicity and it revealed the strongest impairment of T-cell RICD *in vitro*, we focused on TMPA as a Nur77 LBD binding compound for subsequent studies.

TMPA significantly reduced T-cell RICD following PMA but also following TCR crosslinking *via* an agonistic aCD3 antibody. On the other hand, TMPA did not significantly alter T-cell apoptosis induced by agonistic anti FAS antibody (**Figure 4c**). To test, whether TMPA also reduced antigen-specific RICD in primary human T-cells, EBV-specific T-cell blasts were expanded and re-stimulated with an EBV peptide pool to induce RICD. TMPA reduced RICD significantly in EBV peptide pool- and also PMA re-stimulated EBV-specific T-cell blasts (**Figure 4d**).

Taken together, TMPA consistently reduced T-cell RICD in both, polyclonal T-cell blasts and in EBV peptide-specific T-cell blasts. In contrast, FAS mediated, *extrinsic* T-cell blast apoptosis was not altered in the presence *vs.* absence of TMPA treatment, indicating that TMPA specifically blocked TCR-signaling induced, *intrinsic* RICD in primary human T-cells (**Figure 4e**).

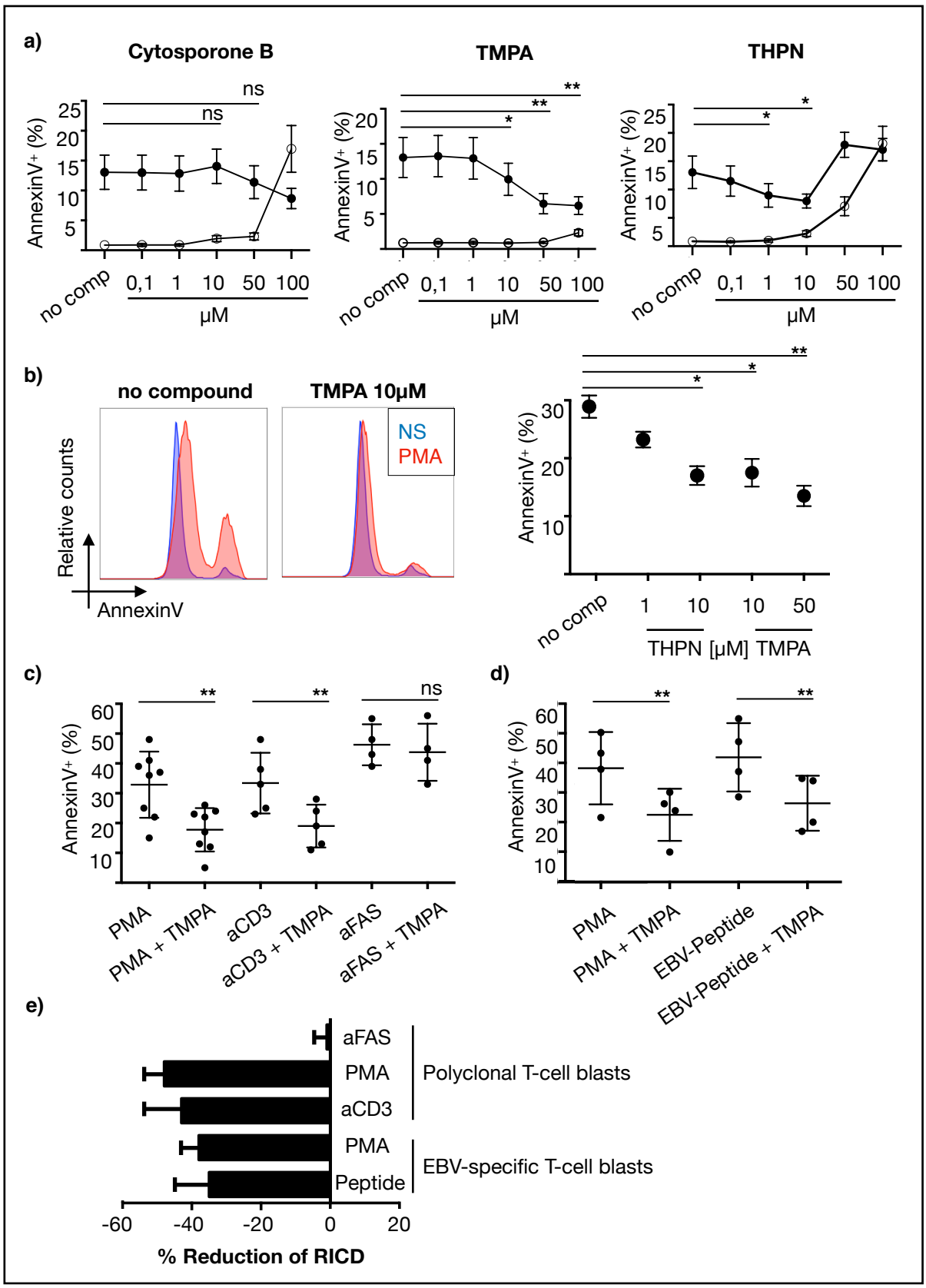

Figure 4 Effect of Nur77-binding small molecule compounds on T-cell RICD

a) - c) Primary human T-cell blasts ((a) N=4, b), c) N=8)) were re-stimulated with PMA, treated with agonistic anti-CD3 monoclonal antibody (clone OKT3), agonistic FAS-specific monoclonal antibody (aFAS) or left unstimulated. Small molecule compounds cytosporone-B, TMPA and THPN were added at the indicated concentrations prior to re-stimulation. In **c**) and **d**) TMPA was used at a concentration of 10 μM. Four hours later, $CD3^+CD8^+$ T-cell blasts were assessed for T-cell RICD using annexinV staining and flow-cytometric analysis according to 2.3.3. In **b**) representative histogram plots of

annexinV fluorescence are depicted together with a summary graph displaying results measured in T-cell blasts derived from individual blood donors **d)** EBV-specific T-cell blasts (N=4) were initially stimulated with an EBV peptide-pool and subsequently flow-sorted for IFNγ positive T-cell blasts. These cells were then *in vitro* re-stimulated using either EBV peptide pool or PMA. Four hours later, T-cell RICD was measured by annexinV staining and flow-cytometric analysis according to 2.3.3. **e)** Relative reduction of T-cell RICD in the presence compared to the absence of 10 μM TMPA is depicted (% of annexinV$^+$ cells in the presence *vs.* absence of Nur77 binding small molecule compounds). All cells were gated for CD3$^+$/CD8$^+$ expression for flow-cytometric analysis of apoptosis. Statistics were performed using two-way- ANOVA test, ns indicates non-significant changes, * = p<0,05, ** = p<0,01, *** = p<0,001. Mean and standard deviation are shown.

3.2.2 TMPA reduces *intrinsic* effector caspase 9 activation, but has no impact on mitochondrial outer membrane potential

The pro-apoptotic function of Nur77 has been reported to depend on its intracellular localization. Several studies described nuclear-cytoplasmic translocation of Nur77 in colon and gastric cancer cells as a prerequisite for apoptosis induction. This translocation was accompanied by association to BH3 and BH4 containing Bcl-2 family members following conformational change that induced mitochondrial depolarization and subsequent cytochrome-C release and caspase 9 activation[115,143,174,175].

To test, whether TMPA impacted on mitochondrial outer membrane permeabilization (MOMP) and effector caspase activation in re-stimulated primary human T-cells, MOMP was visualized during T-cell RICD using the mitochondrial membrane potential dependent fluorescent dye TMRE and flow-cytometric analysis (**Figure 5**).

TMRE staining of primary human T-cell blasts revealed high fluorescence signal in non-re-stimulated cells. PMA- and TCR crosslinking induced T-cell RICD was associated with reduced TMRE fluorescence, indicating MOMP and apoptosis induction (see **Figure 2**). FAS crosslinking was also associated with MOMP, implying that T-cell apoptosis *per se* is associated with MOMP. Unexpectedly, TMPA, applied at concentrations at 10μM or 50μM, did not alter MOMP, while it reduced T-cell RICD (**Figure 5a**). This lack of impacting on MOMP was observed regardless whether the percentage of TMRE^{lo} T-cells or the TMRE mean fluorescence intensity (MFI) was monitored (**Figure 5a**).

Assessment of effector caspase 8 and 9 activation four hours after re-stimulation with titrated PMA concentrations revealed a dose-dependent increase of caspase 9 activation. PMA re-stimulation also led to activation of caspase 8, although caspase 8 activation numerically was lower compared to activation of caspase 9 (**Figure 5b**). TMPA reduced PMA induced caspase 9 activity up to 40% compared to TMPA non-treated, re-stimulated T-cells blasts (**Figure 5b**).

Taken together, TMPA reduced RICD in primary human T-cells. While this was associated with reduced activation of caspase 9, MOMP was insensitive to presence *vs.* absence of TMPA.

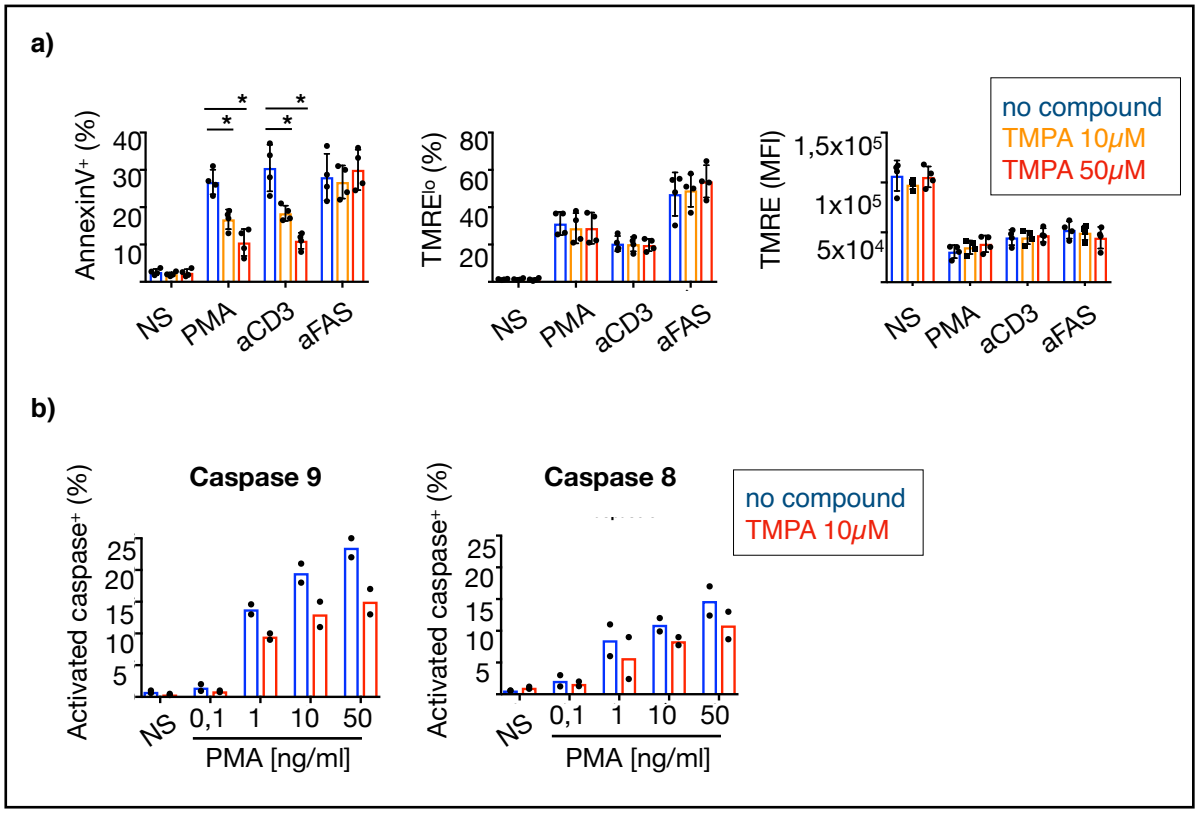

Figure 5 Effect of TMPA on MOMP and activation of effector caspases
a) Primary human T-cell blasts (N=3) were re-stimulated with PMA, treated with agonistic anti-CD3 monoclonal antibody (clone OKT3), agonistic FAS-specific monoclonal antibody (aFAS) or left unstimulated in medium. TMPA was added at the indicated concentrations prior to re-stimulation. Four hours later, $CD3^+CD8^+$ T-cells were assessed for apoptosis using annexinV staining and flow-cytometric analysis according to 2.3.3. For assessment of the mitochondrial potential, the same T-cell blasts were incubated after four hours of re-stimulation for additional 30 minutes at 37°C in medium containing TMRE according to the manufacturers protocol (Immunochemistry technologies). TMRE fluorescence was measured by flow-cytometry. **b)** For assessment of caspase activation, primary human T-cell blasts (N=2) were incubated after four hours of re-stimulation with titrated amounts of PMA for additional 30 minutes at 37°C in medium containing fluorochrome-labeled caspase 8- or caspase 9-specific inhibitors according to the manufacturers protocol (Immunochemistry technologies) before flow-cytometric analysis. The percentage of T-cell blasts displaying activated caspases is depicted.
For flow-cytometric analysis, cells were gated on $CD3^+/CD8^+$. Statistics were done with two-way-ANOVA test, ns indicates non-significant changes, * = p<0,05, ** = p<0,01, *** = p<0,001. Mean and standard deviation are shown.

3.2.3 TMPA does not affect effector functions of primary human T-cell blasts

Following the observation, that TMPA significantly blocked RICD in primary human T-cells, we next tested whether TMPA altered T-cell effector function. Four hours after re-stimulation of human T-cell blasts with PMA or agonistic anti-CD3 antibody, cells were analyzed for intracellular content of TNFα and IFNɣ. While PMA and anti-CD3 rapidly induced TNFα and IFNɣ, presence *vs.* absence of TMPA did not significantly alter the production of both effector cytokines, although a trend to lower cytokine production was observed with high-dose TMPA (50μM) (**Figure 6**).

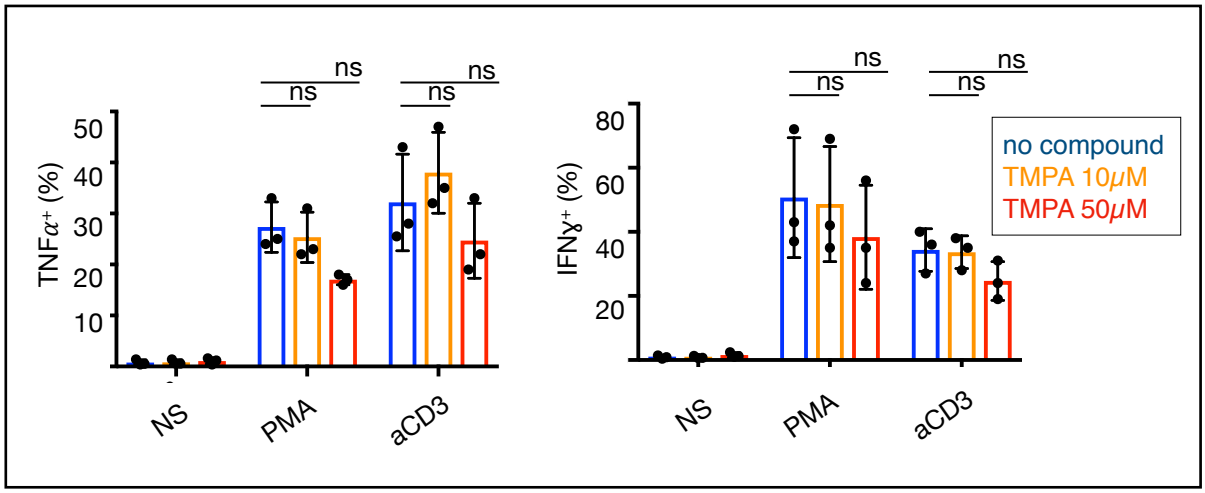

Figure 6 Effect of TMPA on primary human T-cell blast effector function
To assess the effect of TMPA on T-cell blast *intrinsic* effector functions, primary human T-cell blasts (N=3) were re-stimulated with PMA, treated with agonistic anti-CD3 monoclonal antibody (clone OKT3), agonistic FAS-specific monoclonal antibody (aFAS) or left unstimulated in medium. TMPA was added at the indicated concentrations as was Brefeldin-A (5 μg/ml) to block cytokine secretion. After four hours of re-stimulation, flow-cytometric analysis of TNFα or IFNγ expression was performed following intra-cellular cytokine staining according to 2.3.4. Cells were gated for $CD3^+/CD8^+$ for flow-cytometric analysis. Statistics were performed using a two-way-ANOVA test, ns indicates non-significant changes, * = p<0,05, ** = p<0,01, *** = p<0,001. Mean and standard deviation are shown.

3.2.4 Primary human T-cell proliferation in the presence of Nur77 binding small molecule compounds

As TMPA consistently reduced human T-cell RICD, we next tested the effect of TMPA on primary T-cell proliferation (**Figure 7**).

Peripheral blood mononuclear cells (PBMC) were activated with agonistic antibodies against CD3 and CD28 in the presence of IL-2 to induce T-cell expansion. T-cell proliferation was monitored by flow-cytometric tracking of CFSE fluorescence signal loss following T-cell division. Four days after primary stimulation, T-cells showed decreased CFSE fluorescence indicative of functional cell division. TMPA and THPN at low doses (TMPA 10μM, THPN 1μM) revealed no detectable impact on cell division, whereas high doses (TMPA 50μM, THPN 10μM) were associated with inhibition of primary T-cell proliferation (**Figure 7a**).

In a confirmatory experiment, primary T-cell expansion was induced by phytohemagglutinin (PHA) in the presence or absence of IL-2. T-cell activation using anti-CD3/CD28 monoclonal antibodies served as control. Cells were cultured in the presence or absence of 10μM TMPA. T-cell *intrinsic* CFSE signal was monitored by flow-cytometry over the next four following days. PHA, similar to activation by anti CD3/CD28 antibodies, led to CFSE dilution indicative of intact T-cell division. TMPA at the concentrations of 10μM did not affect primary T-cell division (**Figure 7b**).

To test whether constant presence of TMPA during primary T-cell proliferation impaired its effect to reduce RICD (tachyphylaxis), primary T-cells were expanded following PHA stimulation in the presence of IL-2 for seven days. TMPA was added before primary stimulation and every three days (together with fresh IL-2) at a concentration of 10μM. T-cells stimulated in the absence of TMPA served as control. Seven days later, RICD was induced by titrated amounts of PMA, again in the presence *vs.* absence of 10μM TMPA. Independent whether T-cell blasts were expanded in the presence or absence of TMPA, TMPA reduced T-cell *intrinsic* RICD during the four hours of re-stimulation (**Figure 7c**). In other words, we do not have experimental evidence that constant encounter with TMPA leads to tachyphylaxis regarding its potential to reduce T-cell RICD.

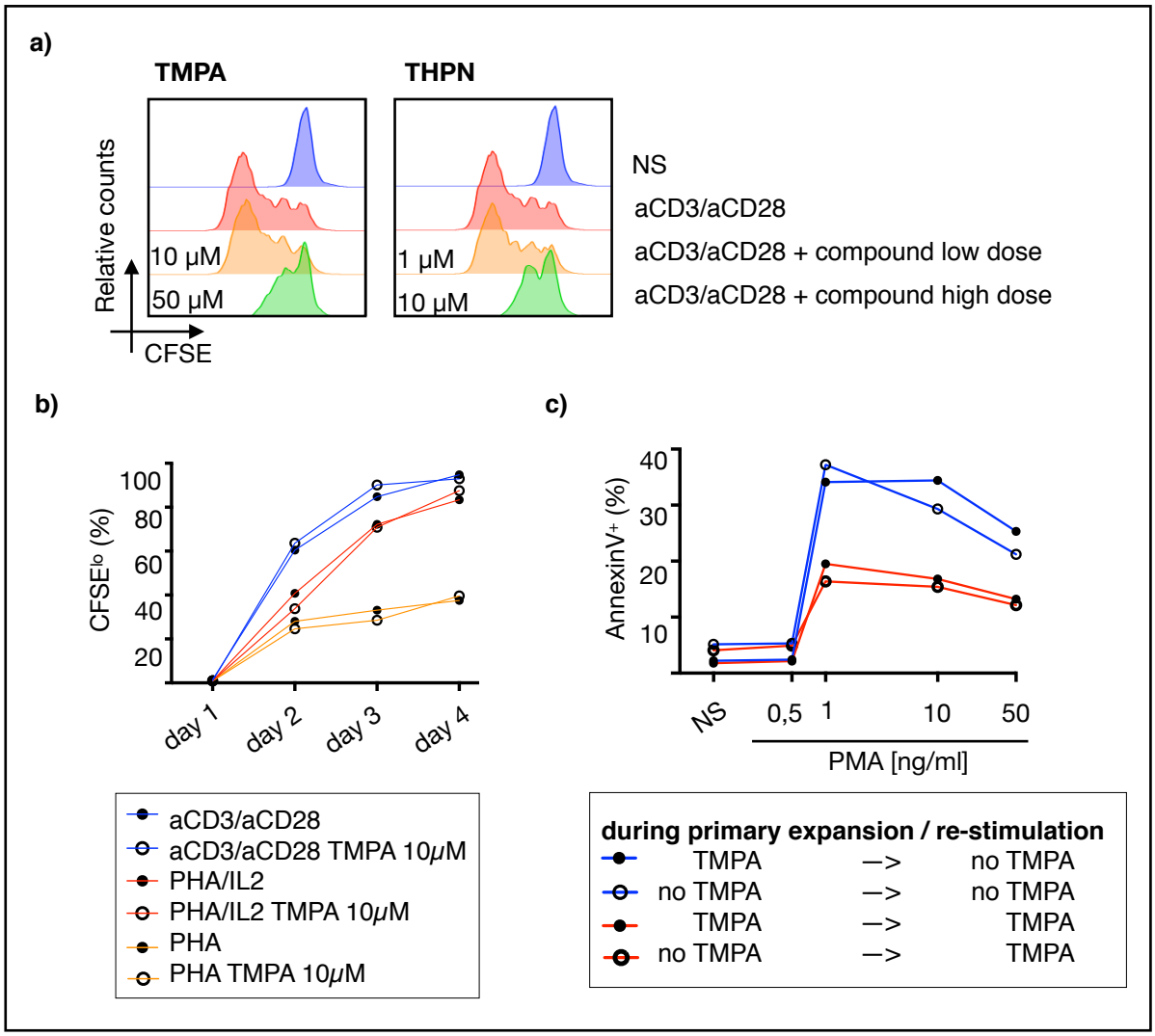

Figure 7 Effect of TMPA and THPN on primary T-cell proliferation
a), b) PBMC were CFSE-labeled according to 2.2.3 (N=2). PBMC derived T-cells were subsequently activated with agonistic monoclonal antibodies against CD3/CD28 or PHA plus IL-2. Non-stimulated conditions served as control. TMPA and THPN were added at the indicated concentrations prior to stimulation. Dilution of CFSE fluorescence as an indicator of cell division was monitored by flow-cytometry after four days (**a**) or at the indicated time points after activation (**b**). All cells were stained for CD3 and CD8 expression and flow-cytometrically gated on $CD3^+/CD8^+$ for analysis. **c)** To analyze whether presence *vs.* absence of TMPA during primary T-cell proliferation impacted on its effect during T-cell RICD, primary human T-cell blasts (N=2) were expanded using PHA plus IL-2 for seven

days in RPMI medium containing or not containing TMPA (10 μM). TMPA was freshly added together with fresh IL-2 after three days of culture. After seven days of primary T-cell expansion, T-cell blasts were re-stimulated using the indicated titrated concentrations of PMA or were left unstimulated, again in the presence *vs.* absence of TMPA (10 μM). Four hours later, T-cell RICD was measured by annexinV staining and flow-cytometric analysis according to 2.3.3. All cells were gated on $CD3^+/CD8^+$ for analysis. Results of individual experiments are shown.

3.3 TMPA reduces TCR mediated RICD in primary murine T-cell blasts

Having shown TMPA to consistently impact on RICD in primary human T-cell blasts, we wanted to test, whether TMPA is also capable of reducing RICD in murine primary T-cells. Therefore, we used TMPA in the context of T-cells isolated from 327^{tg} mice. Almost all $CD8^+$ T-cells derived from 327^{tg} mice express a transgenic TCR specific for the immunodominant LCMV peptide gp33-$41^{164–166}$. These transgenic T-cells allowed us to analyze the function of TMPA in the context of RICD induced by crosslinking the TCR by re-stimulation with the cognate peptide (**Figure 8**).

LCMV-specific $CD8^+$ T-cells were first expanded by *in vitro* incubation with gp33-41 peptide in the presence of IL-2. Eight days later, RICD was induced by re-application of gp33-41 and T-cell apoptosis was assessed by annexinV staining and flow-cytometric analysis four hours later. Unspecific re-stimulation using the ovalbumin derived OVA peptide served as a control and did not result in RICD (**Figure 8a**). TMPA reduced murine T-cell RICD dose-dependently with a similar dose response curve as observed in primary human T-cell RICD (**Figure 8a**).

gp33-41 re-stimulation led to TNFα and IFNγ production in more than 60% of the LCMV-specific T-cell blasts (**Figure 8b**). OVA re-stimulation as a control did not induce cytokine-production in LCMV-specific T-cells. As observed in human primary T-cell blasts, TMPA did not significantly impair cytokine production upon re-stimulation, although a tendency to reduced IFNγ production was observed at a TMPA concentration of 50μM (**Figure 8b**). In line with human T-cell blasts, TMPA was not associated with increased T-cell death under non-re-stimulated conditions (**Figure 8b**).

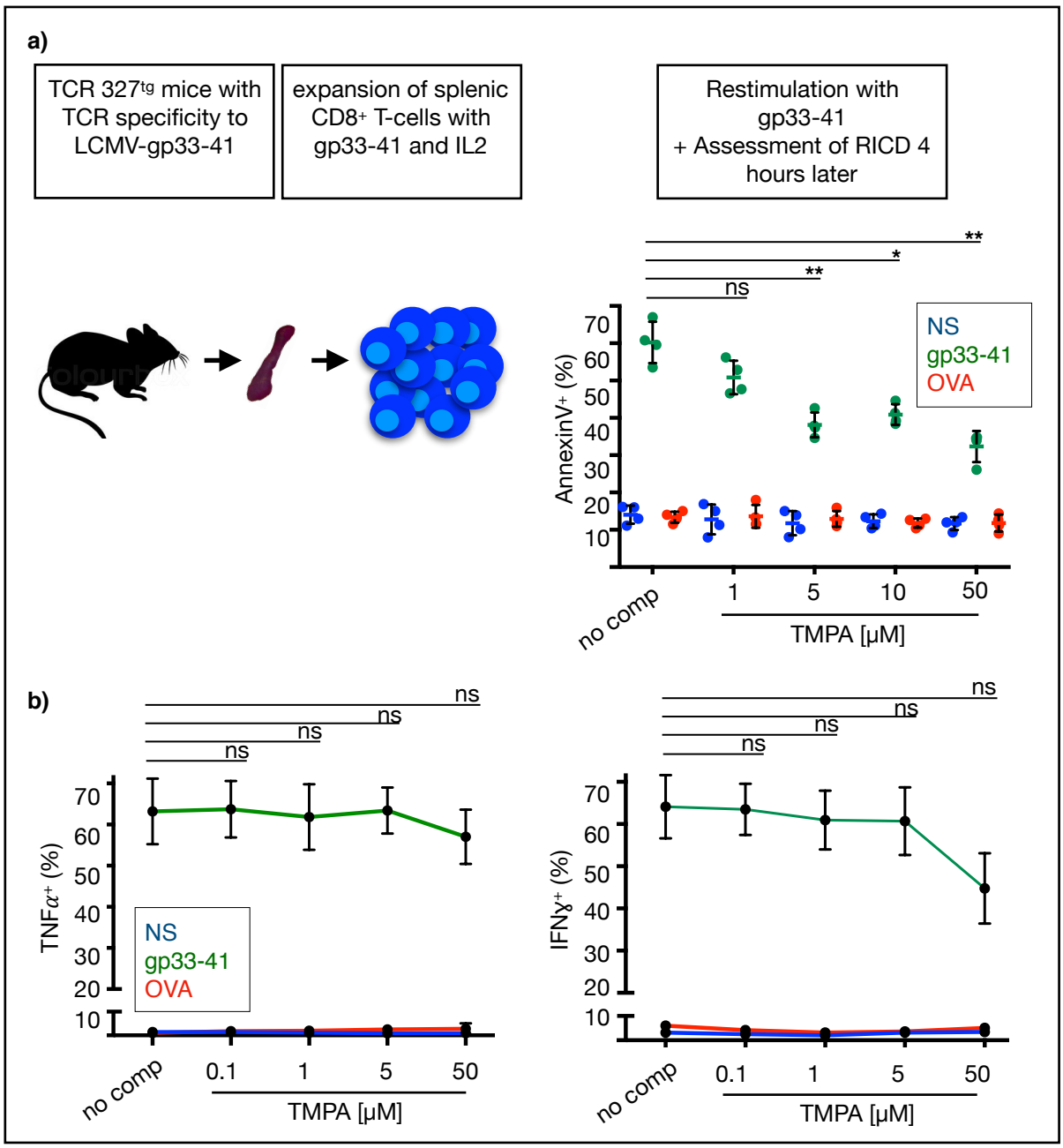

Figure 8 Effect of TMPA on murine T-cell RICD and murine T-cell blast effector functions

a), b) Splenocyte-derived LCMV-specific primary murine T-cell blasts (N=4) were generated using 327^{tg} mice that contain TCR-transgenic CD8^{+} T-cells specific for the immunodominant LCMV-glycoprotein-derived gp33-41 peptide according to 2.1.4. Eight days after initial T-cell expansion using gp33-41 and IL-2, murine T-cell blasts were *in vitro* re-stimulated using gp33-41, ovalbumin-derived OVA peptide or were left unstimulated. TMPA was added at the indicated titrated concentrations prior to re-stimulation. (**a**) Four hours later, T-cell RICD was measured by annexinV staining and flow-cytometric analysis according to 2.3.3. (**b**) T-cell *intrinsic* production of TNFα and Interferonɣ (IFNɣ) was assessed by intracellular cytokine staining and flow-cytometric analysis. Brefeldin-A (5 µg/ml) was used to block cytokine secretion during the re-stimulation cultures.
All cells were gated on CD3^{+} for flow-cytometric analysis. Statistics were done with two-way-ANOVA test, ns indicates non-significant changes, * = p<0,05, ** = p<0,01, *** = p<0,001. Mean and standard deviation are shown.

3.4 Analysis of T-cell RICD associated transcriptomes in the presence *vs.* absence of TMPA

Our previous experiments substantiated the function of Nur77 binding small molecule compounds to reduce T-cell *intrinsic* RICD in both murine and human T-cell blasts. To gain insight into how TMPA might mechanistically regulate T-cell RICD, we performed RNA sequencing experiments (**Figure 9**).

3.4.1 Identification of a distinct differentially regulated, TMPA sensitive small set of genes in re-stimulated primary T-cells

For RNA sequencing, splenocyte derived T-cell blasts from four 327^{tg} mice were first expanded and subsequently re-stimulated with gp33-41 peptide. Processing of individual mice, T-cell expansion and RICD induction was performed individually to augment statistical power. To also get information on dose-dependent TMPA effects on gene transcription during T-cell RICD, RNA sequencing was performed on murine T-cell blasts re-stimulated in the presence of 5μM and 50μM TMPA, respectively. Besides non-re-stimulated T-cell blasts, unspecific re-stimulation with OVA peptide served as an additional control. As OVA re-stimulated T-cell blasts did not reveal significant differences in mRNA regulation compared to non-re-stimulated cells, non-stimulated (NS) and OVA stimulated (OVA) conditions could be merged and used as a combined control throughout the analysis of the RNA sequencing data. This generated a higher statistical power for the definition of significant TMPA related changes in gene regulation during T-cell RICD.

Clustering analysis of all samples demonstrated, that the generated dataset was valid and robust, as the samples showed low differential gene regulation within the re-stimulated and the control conditions, respectively. Also, no major differences regarding gene transcription between individual mice were observed, whereas comparison of gp33-41 re-stimulated with non-re-stimulated conditions revealed major differential gene regulation (**Figure 9a**).

Principal component analysis of the generated data set showed, that the majority of the differential gene regulation (94,47% - principal component x) emerged from TCR crosslinking induced re-stimulation, indicating a (expected) major gene regulation due to re-stimulation itself. However, presence *vs.* absence of TMPA in re-stimulated samples also revealed a dominant parameter for differential gene regulation (3,9% - principal component y). Plotting of both principal component parameters x and y demonstrated, that the gp33-41 re-stimulated samples cluster together. Within re-stimulated T-cell blasts, TMPA treated *vs.* non-treated samples cluster separately together, visualizing a distinct impact of TMPA treatment on gene regulation in LCMV-specific re-stimulated primary T-cells blasts (**Figure**

9b). A TMPA related dose dependency could not be observed with this kind of analysis (**Figure 9b**).

A detailed analysis of TMPA-related differential gene regulation by comparing RNA profiles in gp33-41 re-stimulated samples was performed. Statistical cutoffs were defined to evaluate the most significant regulated genes in the datasets. A stringent cutoff with a corrected p-value (FDR) below 0,0005 and a log^2 fold change (log^2 FC) higher than 2,5 or lower than -2,5 was applied. This evaluation revealed a gene set of 41 genes that were differentially regulated during gp33-41 peptide re-stimulation in a TMPA-dependent manner. Notably, 4 of these 41 genes belonged to the gene family encoding for proteins of the Slam receptor signaling axis (**Figure 9c**). One of these gene products, SAP is associated with x-linked lymphoproliferative disease (XLP). XLP is caused by loss of function (LOF) mutations in the *SH2D1A* gene, encoding for SAP[176,177]. It is noteworthy, that SAP deficiency has been reported to reduce RICD in human T-cell blasts[66] comparable to what was observed during RICD in the presence of TMPA and THPN treatment. Therefore, the observed TMPA-dependent regulation of *Sh2d1a* / SAP during T-cell RICD got into our focus of subsequent experimental studies.

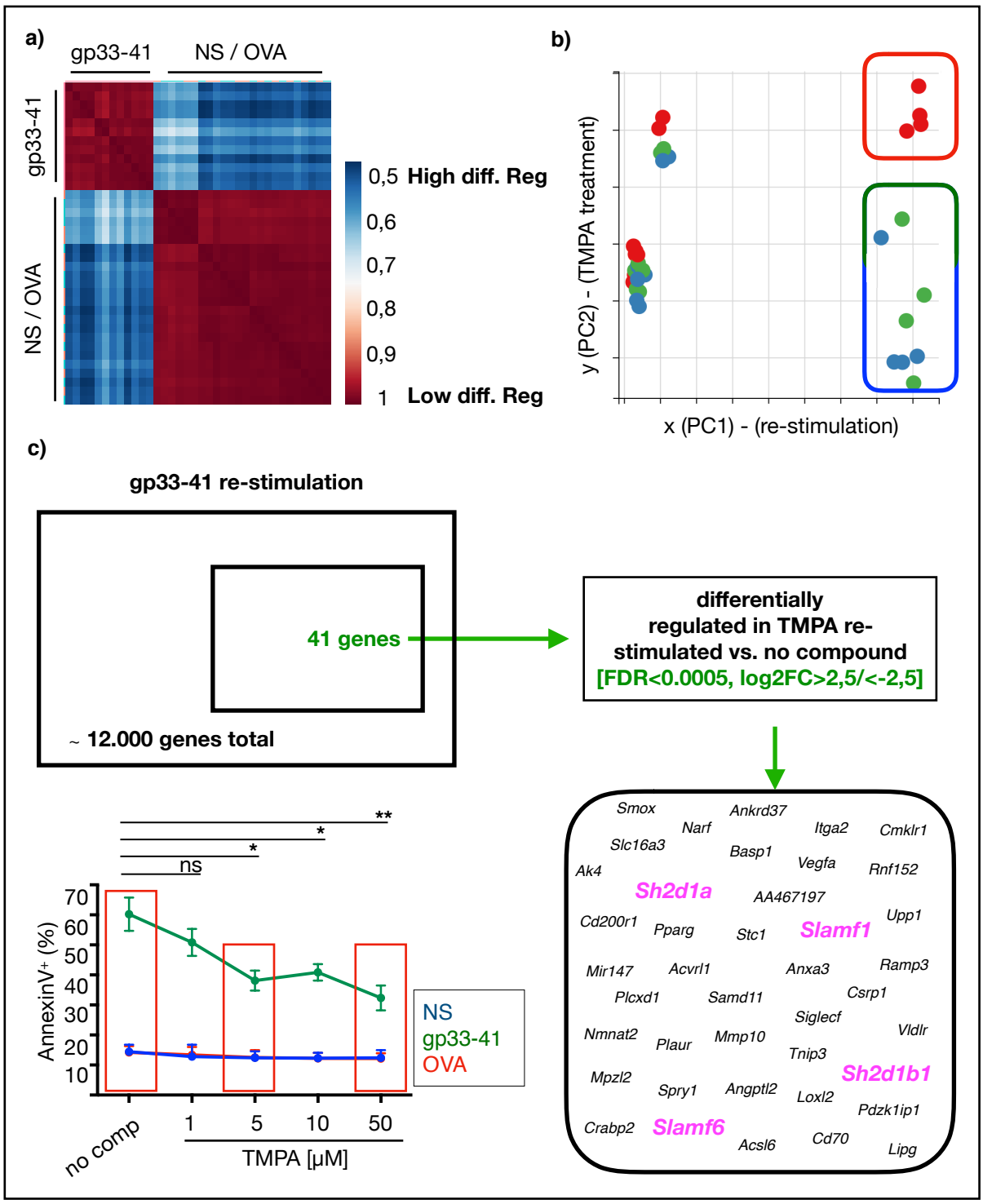

Figure 9 Effect of TMPA on mRNA regulation during T-cell RICD

(**a-c**) Splenocyte-derived LCMV-specific primary murine T-cell blasts (N=4) were generated from 327^{tg} mice that contain transgenic $CD8^{+}$ T-cells specific for the immunodominant LCMV-glycoprotein-derived gp33-41 peptide according to 2.1.4. Eight days following initial T-cell expansion using gp33-41 peptide plus IL-2, murine T-cell blasts were *in vitro* re-stimulated using gp33-41, ovalbumin-derived OVA peptide or left unstimulated in medium. TMPA was added at the indicated final concentrations prior to re-stimulation. Four hours later, T-cell blasts were either assessed for T-cell RICD with annexinV staining and flow-cytometric analysis according to 2.3.3 or replicates of the same T-cell blasts were lysed for subsequent RNA sequencing with special lysis buffer (Machery-Nagel). **a)** A heatmap of all sequenced samples in a cluster analysis regarding transcriptional regulation is depicted. Non-re-stimulated (NS) and non-specifically peptide re-stimulated (OVA) samples were merged, since transcriptional regulation of these two control groups did not statistically differ (data not

shown). Every sample is compared with each other and attributed with a differential gene regulation score between 0,5 (high differential gene regulation) and 1 (low differential gene regulation).
b) Principal component analysis of all sequenced samples is depicted. Principal component parameter 1 (PC1, x-axis, re-stimulation) explains 94,47% of all differential regulated genes. Principal component 2 (PC2, y-axis, TMPA treatment) explains 3.9 % of all differential regulated genes. RNA sequencing data revealed clustering of re-stimulated non-TMPA treated (red dots) samples *vs.* re-stimulated TMPA treated samples (blue and green dots) regarding differential gene regulation.
c) T-cell blasts were either monitored for RICD using annexinV staining and flow-cytometry according to 2.3.3 or cells were lysed four hours after re-stimulation and RNA sequencing was performed (see 2.5). Highly differential regulated genes in re-stimulated TMPA-treated *vs.* re-stimulated non-TMPA treated samples are depicted. Genes belonging to the Slam receptor signaling axis are highlighted in purple.
Statistics were performed using two-way-ANOVA test, ns indicates non-significant changes, * = $p<0,05$, ** = $p<0,01$, *** = $p<0,001$. Mean and standard deviation are shown.

3.4.2 TMPA-dependent regulation of *Sh2d1a* / SAP during RICD in primary murine and human T-cell blasts

Log^2 relative expression of *Sh2d1a* in murine LCMV-specific T-cell blasts that were analyzed for the RNA sequencing experiments are depicted in **Figure 10a.** *Sh2d1a* mRNA was expressed constitutively in non-re-stimulated T-cell blasts (NS) and unspecific (OVA) peptide re-stimulated T-cell blasts. Re-stimulation of LCMV-specific T-cell blasts with cognate gp33-41 peptide did not change *Sh2d1a* mRNA expression, while gp33-41 peptide re-stimulation in the presence of TMPA (both, low (5μM) and high dose (50μM)) led to profound reduction of *Sh2d1a* mRNA expression (**Figure 10a**). Further analyses in primary human T-cells were performed to test whether the regulation of *SH2D1A* and its gene product SAP by TMPA during T-cell RICD was consistent in different species (**Figure 10**).

In keeping with the results in antigen-specific murine T-cell blasts, *SH2D1A* mRNA expression, as assessed by real-time PCR, was reduced during human T-cell RICD in a TMPA-dependent manner (**Figure 10b**). While *SH2D1B1* and *SLAMF6* mRNA showed no TMPA-dependent regulation during human T-cell RICD, *SLAMF1* mRNA expression was significantly increased in the presence of TMPA during T-cell RICD (**Figure 10b**). Thus, the TMPA-dependent regulation of members of the SLAM receptor signaling axis observed during RICD of LCMV-specific transgenic murine T-cell blasts was experimentally recapitulated in primary human T-cell RICD.

Consistent with *SH2D1A* mRNA regulation during human T-cell RICD, SAP protein was downregulated in a TMPA-dependent manner during primary human T-cell RICD within four hours (**Figure 10c**). As a control, apoptosis induction in human T-cell blasts by recombinant soluble FAS ligand (FASL) did not alter T-cell *intrinsic* SAP expression independently of TMPA treatment. Isotype control antibody confirmed specificity of the flow-cytometric quantification of SAP (**Figure 10c**). In summary, *Sh2d1a/SH2D1A* mRNA and SAP protein appeared to be downregulated during T-cell RICD in a TMPA-dependent manner..

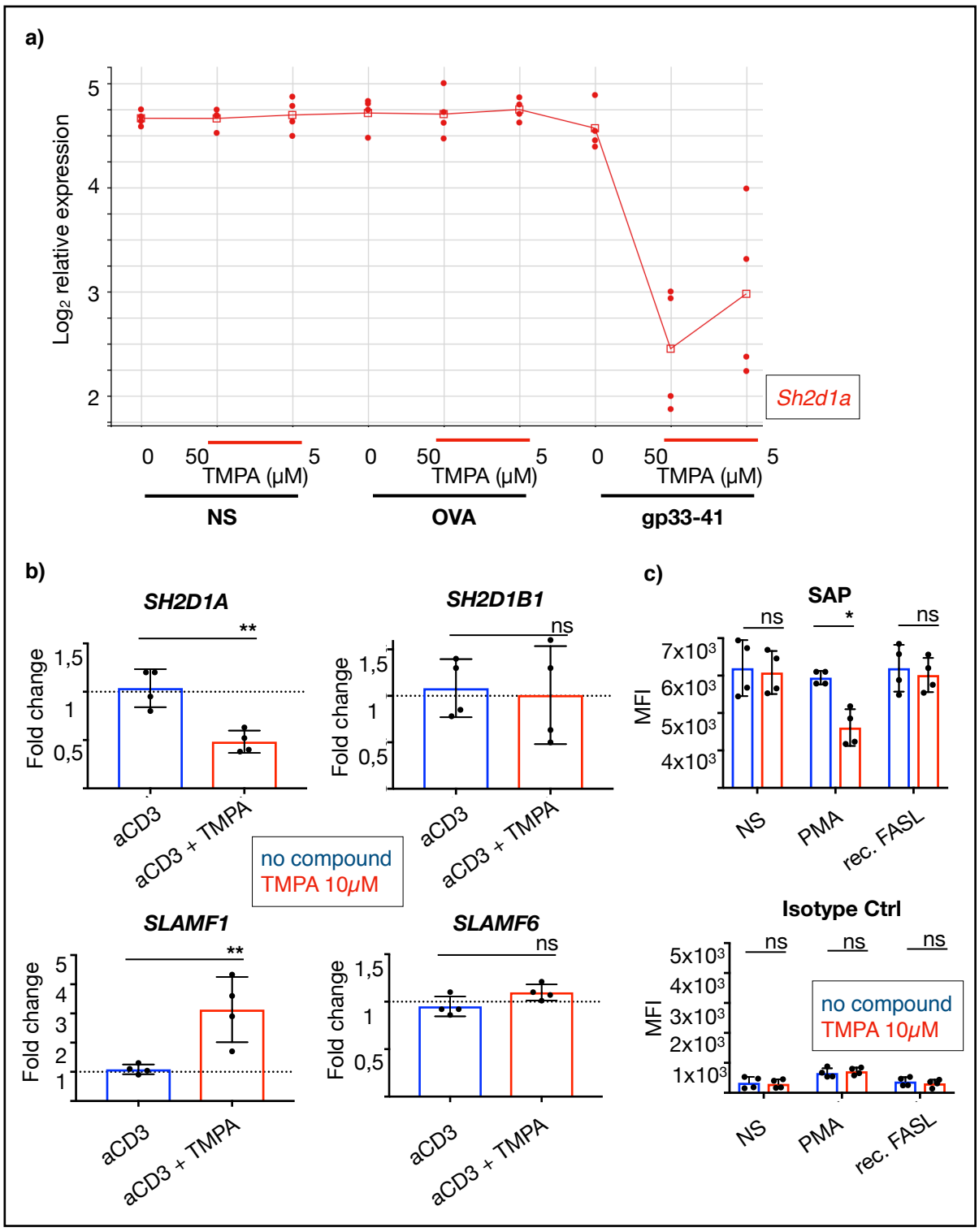

Figure 10 Effect of TMPA on *Sh2d1a* mRNA / SAP protein levels during T-cell RICD
a) RNA sequencing raw data were analyzed for Log² relative expression of *Sh2d1a* (gene encoding for SAP) in all indicated 9 re-stimulation conditions (N=4) (see **Figure 9**) using an in-house analysis tool (bioinformatics core facility of the Department of Biomedicine Basel). For re-stimulation, splenocyte derived primary murine LCMV-specific T-cell blasts were re-stimulated using LCMV peptide gp33-41, ovalbumin-derived OVA peptide or were left unstimulated. TMPA was directly added at the indicated concentrations prior to re-stimulation. RNA was isolated after four hours of re-stimulation. **b)** Primary human T-cell blasts (N=4) were re-stimulated with agonistic anti CD3-specific monoclonal antibody (clone: OKT3) or left unstimulated in medium in the presence *vs.* absence of TMPA (10 µM). mRNA expression of *SH2D1A*, *SH2D1B1*, *SLAMF1* and *SLAMF6* was assessed by quantitative PCR after four hours of re-stimulation according to 2.4.3. All mRNA expression values are normalized to housekeeping genes *18s* and *Ipo8*. The depicted fold change values are normalized to

mRNA expression in non-stimulated conditions. **c)** Primary human T-cell blasts (N=4) were *in vitro* re-stimulated with PMA, treated with soluble recombinant FASL or were left unstimulated in presence *vs.* absence of TMPA (10 μM). SAP expression was measured using intracellular-staining and flow-cytometric analysis four hours after re-stimulation according to 2.3.4. IgG1 κ isotype control was used as an isotype control. Individual MFI values are depicted. Mean and standard deviation are shown. Statistics were performed using two-way-ANOVA test, ns indicates non-significant changes, * = p<0,05, ** = p<0,005, *** = p<0,0005. Mean and standard deviation are shown.

3.5 Effect of TMPA on T-cell RICD and T-cell effector functions in Nur77 deficient T-cells

Experiments in both primary human and murine T-cells demonstrated a consistent impairment of RICD in the presence of the Nur77 binding small molecule TMPA. Since these compounds had been demonstrated to induce apoptosis in various cancer cell lines[94,95] and hepatocytes[96], we next assessed whether the observed apoptosis inhibiting effect by these Nur77 binding compounds in T-cells was depending on Nur77 expression. For this purpose, Nur77 deficient *Nr4a1*$^{-/-}$ mice[81,148,154] were crossed to 327^{tg} mice. This allowed us to experimentally address the question, whether TMPA related impairment of T-cell RICD required Nur77 protein (**Figure 11**).

3.5.1 TMPA reduces T-cell RICD Nur77-independently

Log^2 relative expression of all 3 NR4A members *Nr4a1*, *Nr4a2* and *Nr4a3* from the RNA sequencing datasets of re-stimulated primary murine T-cell blasts confirmed rapid, early mRNA induction of *Nr4a1*, encoding for Nur77. The other two NR4A gene family members *Nr4a2* and *Nr4a3* encoding for Nurr1 and Nor1, respectively, were also rapidly induced during murine T-cell RICD (**Figure 11a**).

We next expanded LCMV-specific T-cell blasts that were either Nur77 deficient or Nur77 competent using splenocytes from either 327^{tg}xNur77$^{-/-}$ or 327^{tg}xNur77$^{+/-}$ or 327^{tg}xNur77$^{+/+}$ mice. Flow-cytometric analysis two hours following re-stimulation with gp33-41-peptide demonstrated that Nur77 upregulation was similar in Nur77$^{+/-}$ *vs.* Nur77$^{+/+}$ T-cell blasts, whereas Nur77 was indeed absent in Nur77$^{-/-}$ T-cell blasts (**Figure 11b**).

Assessment of T-cell RICD by annexinV staining and flow-cytometric analysis four hours after gp33-41 peptide re-stimulation demonstrated RICD in approximately 60% of LCMV-specific T-cell blasts, regardless of Nur77 competence (**Figure 11c**). Non-re-stimulated T-cell blasts served as control and demonstrated absence of RICD. TMPA was associated with a significant and dose-dependent reduction of RICD, both in Nur77 competent but also similarly in Nur77 deficient T-cell blasts (**Figure 11c**). Together, this experimental evidence implicated that Nur77 expression is not required for the RICD inhibiting effect of TMPA in primary murine T-cell blasts (**Figure 11c**). In addition to the flow-cytometric assessment of

Nur77, we also measured *Nr4a1* and *Nr4a3* mRNA induction during Nur77 competent *vs.* Nur77 deficient T-cell RICD by real-time PCR. Consistent with flow-cytometric assessment of Nur77 expression, re-stimulation of LCMV-specific T-cell blasts with gp33-41 peptide revealed strong induction of *Nr4a1* in Nur77 competent T-cells (3000 fold increase), but not in Nur77 deficient T-cells. Following T-cell blast re-stimulation, also *Nr4a3* mRNA expression was highly induced, notably with a non-significant trend to augmented induction in Nur77 deficient T-cell blasts (**Figure 11d**). Thus, while Nur77 was not required for the RICD inhibiting properties of TMPA, we cannot exclude that in the absence of Nur77, upregulation of other NR4A family members might have functionally compensated for absent Nur77.

3.5.2 RICD associated T-cell effector functions are sustained by TMPA independently of Nur77 expression

To test, whether TMPA impacted on T-cell effector function during murine T-cell RICD, and whether this occurred Nur77-dependently, Nur77 competent *vs.* deficient LCMV-specific T-cell blasts were assessed for TNFα and IFNγ production four hours after *in vitro* re-stimulation with gp33-41 peptide. TNFα as well as IFNγ were rapidly induced in re-stimulated LCMV-specific T-cell blasts regardless of Nur77 expression (**Figure 11e**). TMPA treatment with low dose (10μM) did not affect cytokine production, whereas high dose (50μM) TMPA was associated with non-significantly reduced T-cell *intrinsic* cytokine production (**Figure 11e**).

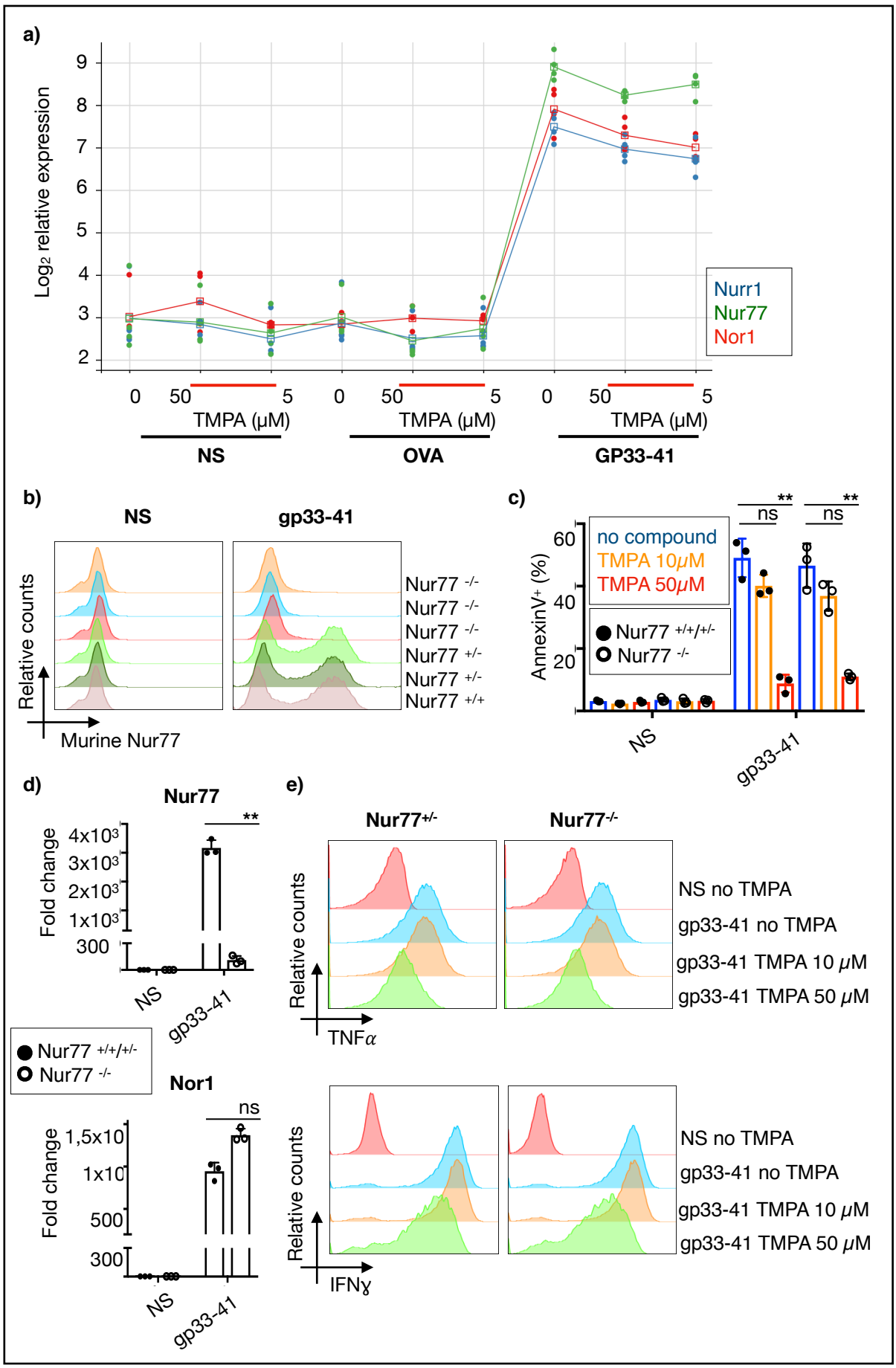

Figure 11 Effect of TMPA on T-cell RICD and T-cell effector functions in Nur77 competent *vs.* deficient T-cells

a) RNA sequencing raw data were analyzed for Log2 relative expression of *Nr4a1*, *Nr4a2* and *Nr4a3* (genes encoding for Nur77, Nurr1 and Nor1) in all indicated 9 re-stimulation conditions (N=4) (see **Figure 9**). **b-e)** Murine $CD8^+$ T-cell blasts specific for the LCMV-peptide gp33-41, either Nur77 competent of Nur77 deficient, were generated using splenocytes from $327^{tg}xNur77^{-/-}$ mice (N=3) and from $327^{tg}xNur77^{+/-}$ or $327^{tg}xNur77^{+/+}$ (N=3) mice and stimulation with gp33-41 peptide plus IL-2. **b)** Fourteen days later, Nur77 expression was assessed by flow-cytometry following re-stimulation with gp33-41 for two hours. Non-stimulated T-cell blasts served as control. Flow cytometry was performed according to 2.3.4. **c)** Sixteen days following initial stimulation, LCMV-specific T-cell blasts were *in vitro* re-stimulated with the LCMV-derived peptide gp33-41 or left unstimulated in the presence *vs.* absence of the indicated concentration of TMPA prior to re-stimulation. Apoptosis was measured by annexinV staining and flow-cytometric analysis according to 2.3.3. four hours after re-stimulation **d)** Sixteen days following generation of T-cell blasts, cells were re-stimulated using gp33-41 (1 nM) or left unstimulated. Four hours later, mRNA expression levels of *Nr4a1* and *Nr4a3* were measured by quantitative PCR according to 2.4.3. All mRNA expression values are normalized to housekeeping genes *18s* and *Ipo8*. Fold change values normalized to non-re-stimulated conditions are depicted. **e)** Eighteen days following generation of LCMV-specific T-cell blasts, T-cell RICD was induced using LCMV-derived peptide gp33-41 (1 nM) or T-cell blasts were left unstimulated in the presence *vs.* absence of the indicated concentration of TMPA. Four hours later, T-cell *intrinsic* production of TNFα and Interferonγ (IFNγ) was assessed by intracellular cytokine staining and flow-cytometric analysis. Brefeldin-A (5 μg/ml) was used during the four hours of re-stimulation to prevent cytokine secretion.
Statistics were performed using two-way-ANOVA test, ns indicates non-significant changes, * = $p<0,05$, ** = $p<0,01$, *** = $p<0,001$. Mean and standard deviation are shown.

3.5.3 TMPA impairs RICD Nur77-independently in primary human T-cells

To test, whether the observed Nur77 independence of the TMPA mediated impairment of murine T-cell RICD was consistently observed in human T-cell RICD, *Nur77* expression was knocked down by transfection of human T-cell blasts with *NR4A1*-specific *vs.* non-specific siRNA (**Figure 12**). 24 hours after transfection, T-cell blasts were enriched for live cells using a magnetic bead based dead-cell removal procedure (see methods). Re-stimulation by TCR crosslinking with an agonistic anti-CD3 antibody induced RICD in 60% of T-cell blasts independently of Nur77 siRNA knock-down. Flow cytometric assessment two hours following re-stimulation demonstrated almost complete abrogation of Nur77 protein expression in Nur77-specific siRNA treated T-cell blasts (**Figure 12**). Thus, Nur77-independence of the TMPA regulated RICD was experimentally shown both in primary murine and primary human T-cell blasts.

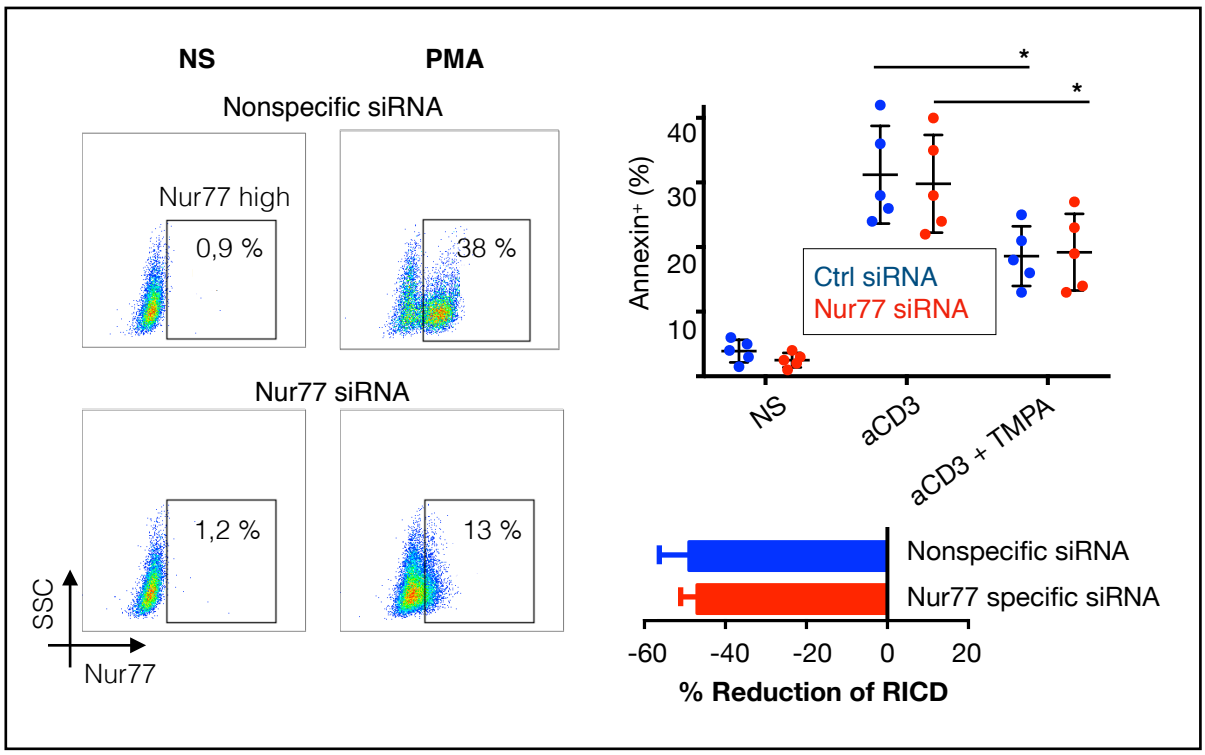

Figure 12 Effect of TMPA on RICD in Nur77 competent *vs.* deficient primary human T-cell blasts

Primary human T-cells blasts (N=5) were transfected by electroporation with *NR4A1*-specific siRNA or non-specific siRNA according to 2.2.2. T-cell blasts were then rested for 24 hours and subsequently enriched for live cells using a magnetic bead-based dead cell removal procedure according to the manufacturer's protocol. Subsequently, T-cell blasts were *in vitro* re-stimulated with PMA or left unstimulated in the presence *vs.* absence of TMPA (10 μM). Four hours later, apoptosis was monitored using annexinV staining and flow-cytometric analysis according to 2.3.4 Quantification of apoptosis in all 5 individual T-cell blast samples is depicted.
To control for Nur77 protein knock-down efficiency, Nur77 expression was assessed two hours after PMA triggered re-stimulation using flow-cytometry. Flow-cytometric Nur77 staining of non-re-stimulated T-cell blasts served as a control. Histograms from one representative experiment are depicted. A summary graph shows the TMPA driven reduction of T-cell RICD in Nur77 competent *vs.* Nur77 deficient primary human T-cell blasts (mean of N=5 is depicted).
For flow-cytometric analysis, all cells were gated on $CD3^+/CD8^+$. Statistics were done with two-way-ANOVA test, ns indicates non-significant changes, * = p<0,05, ** = p<0,01, *** = p<0,001. Mean and standard deviation are shown.

3.6 Nur77-dependent down-regulation of *Sh2d1a* mRNA during T-cell RICD by TMPA

RNA sequencing in re-stimulated LCMV-specific T-cell blasts demonstrated TMPA-dependent *Sh2d1a* down-regulation (**Figure 10**). TMPA-dependent *Sh2d1a* down-regulation was confirmed during human T-cell RICD.

To test, whether TMPA mediated, RICD associated *Sh2d1a* down-regulation occurs Nur77-dependently, *Sh2d1a* mRNA expression was assessed by quantitative PCR during RICD of Nur77 competent *vs.* deficient murine LCMV-specific T-cell blasts (**Figure 13**). *Sh2d1a* mRNA was constitutively expressed in non-re-stimulated T-cell blasts regardless of Nur77 expression. Re-stimulation with gp33-41 peptide in the absence of TMPA did not affect

Sh2d1a mRNA expression (**Figure 13**). In contrast, TMPA at low dose (10μM) and high dose (50μM) decreased mRNA expression of *Sh2d1a* by 50% in a Nur77-dependent manner (**Figure 13**). As a control, TMPA did not alter S*h2d1a* mRNA expression in non-re-stimulated, both Nur77 competent and -deficient T-cells (**Figure 13**).

These results implied that in contrast to the TMPA-dependent impairment of T-cell RICD, the TMPA associated reduction of *Sh2d1a* mRNA expression during T-cell RICD required expression of Nur77 and could not be compensated by other NR4A family members.

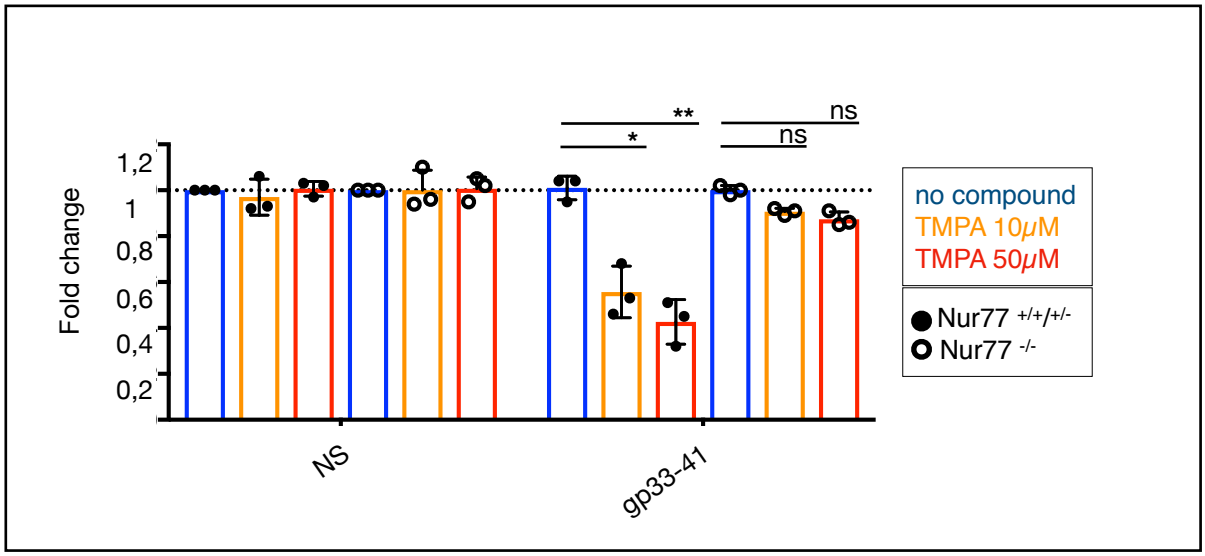

Figure 13 Effect of TMPA on *Sh2d1a* mRNA expression during RICD in Nur77 competent *vs.* deficient primary murine T-cell blasts

Splenocyte-derived LCMV-specific primary murine T-cell blasts were generated from Nur77 deficient 327^{tg}x$Nur77^{-/-}$ mice (N=3) and from Nur77 competent 327^{tg}x$Nur77^{+/-}$ or 327^{tg}x$Nur77^{+/+}$ (N=3) mice by stimulation with LCMV-derived gp33-41 peptide (1nM) plus IL-2 according to 2.1.4.

Eight days later, LCMV-specific T-cell blasts were re-stimulated with LCMV gp33-41 peptide or left unstimulated in the presence *vs.* absence of TMPA at the indicated concentrations. Four hours later, *Sh2d1a* mRNA expression levels were measured by quantitative PCR. mRNA expression values are normalized to the housekeeping genes *18s* and *Ipo8*. The depicted fold change values are normalized to RNA levels measured in non-re-stimulated T-cell blasts.

Statistics were performed with two-way-ANOVA test, ns indicates non-significant changes, * = p<0,05, ** = p<0,01, *** = p<0,001. Mean and standard deviation are shown.

4 Discussion

Biological roles of Nur77 have been extensively experimentally addressed in various cell contexts *in vitro* and *in vivo*. Currently, NCBI search using the terms “Nur77” and “*NR4A1*” yield 1161 and 1121 results, respectively. In my PhD thesis we have Nur77 related functions during RICD of primary mature T-cells and have analyzed effects of pharmacological modulation of Nur77. To our knowledge, this is the first work demonstrating that pharmacological targeting of Nur77 decreases RICD in primary mature murine and human T-cells. This finding reveals a high potential of these Nur77 targeting compounds or pharmacological derivatives to be used to treat diseases linked to dysregulated T-cell apoptosis.

4.1 Nur77 regulates apoptosis *via* different mechanisms depending on the cellular context.

The nuclear orphan receptor Nur77 was initially discovered as an early induced gene in response to serum- or nerve growth factor (NGF) in a pheochromocytoma rat cell line PC12[178,179]. Despite early discovery, that rapid induction of Nur77 is associated with apoptosis in T-cell hybridomas [82,145], the underlying mechanisms remained controversial. Structural analysis of Nur77 revealed a composition similar to other nuclear receptors such as the nuclear steroid receptor[79]. Accordingly, Nur77 contains three main functional domains, consisting of a DNA binding domain (DBD) regulating gene transcription, a transactivation domain (AF-1) and an atypical ligand binding domain (LBD) attributing Nur77 a special role among the nuclear receptors. The rather unusual accumulation of tightly packed hydrophobic residues inside the Nur77-LBD argued against the dependency on natural occurring ligands and proposed Nur77 to act as a ligand-independent constitutively active transcription factor[180,181] A high degree of homology can be observed when analyzing the 3 members of the NR4A family, suggesting certain functional redundancy. This is in keeping with the finding, that while thymocytes from transgenic mice overexpressing a dominant negative form of Nur77 were protected from activation induced cell death[146], Nur77 deficient mice showed no alteration of TCR induced apoptosis suggesting functional compensation through Nurr1 and/or Nor1[81]. Consistently, our results demonstrate an unimpaired T-cell RICD in Nur77 deficient mature murine T-cells. Similarly, siRNA mediated knockdown of Nur77 argued against a unique requirement of Nur77 during mature human T-cell RICD.

The various pro-apoptotic mechanisms of Nur77 have been extensively investigated in cancer research[156,182,183]. Beside the initial discovery of Nur77 to promote cancer cell apoptosis *via* transcriptional gene induction in solid tumor cell lines, other experimental

evidence proposed Nur77 to promote apoptosis *via* posttranscriptional modifications like phosphorylation or SUMOylation[87,161,184,185] and *via* non-genomic trans-repression mechanisms by binding to and inactivating anti-apoptotic Bcl-2 protein family members following nuclear export[140,143,150,161,182,185,186]. Several studies suggested fundamental differences of Nur77 driven functions in immature *vs.* mature T-cells. Whereas Nur77 induction promoted clonal deletion during negative selection of thymocytes, it was found to drive proliferation and survival in mature, peripheral T-cells[25,86,144,151,187].

In mature, re-stimulated T-cell blasts, our results demonstrate rapid Nur77 up-regulation during RICD. In line with the findings of Cunningham and colleagues[25,151], we did not find experimental evidence of Nur77 nuclear export during re-stimulation of both primary murine and human T-cell blasts using a recently developed device that combines flow-cytometric analysis with fluorescence microscopy and brightfield imaging (Image Stream X®, Merck Milipore, data not shown). Future studies using T-cell adapted nuclear *vs.* cytosolic fractionation methods and western-blot analysis will allow to study whether Nur77 nuclear export occurs during mature T-cell RICD and may elucidate its relevance.

4.2 Modulation of T-cell RICD by Nur77 binding small molecule compounds

The apoptosis-related functions of Nur77 revealed a high potential for being drug-targeted in cancer therapy. Since no natural occurring ligand of Nur77 has been described, several natural-occurring or synthetic small molecule compounds binding to the hydrophobic amino residues within the Nur77-LBD, have been described to alter the biology of cancer cells or hepatocytes in a Nur77-dependent manner[93–96,162]. Here we applied some of these compounds for the first time during primary expansion and RICD of mature T-cells. While cytosporone-B and THPN (1-(3,4,5-trihydroxyphenyl)nonan-1- one) were reported to induce apoptosis in tumor cell lines and in tumors *in vivo via* driving nuclear export of Nur77, TMPA (ethyl [2,3,4-trimethoxy-6-(i-octanoyl) phenyl]acetate) was shown to reduce blood glucose levels in diabetes-prone mice[96]. Its anti-tumor effects and its impact on Nur77-associated apoptosis and nuclear export have not been addressed yet. Application of these Nur77 binding small molecules to mature primary T-cell blasts revealed a rather unexpected albeit consistent reduction of RICD, given that these compounds were reported to induce apoptosis.

4.2.1 Nur77 binding small molecule compounds impair TCR induced RICD in mature T-cells

Our experiments demonstrated that human T-cell RICD occurred MEK/ERK-dependently. Reduced phosphatidylserine exposure following re-stimulation in the presence of MEK inhibitors correlated with reduced caspase 9 activation. In contrast to cancer cell lines and hepatocytes, T-cells do not show constitutive expression of Nur77. However, re-stimulation of mature T-cell blasts was followed by rapid Nur77 induction, which was prevented by MEK inhibition. Notably, we did not observe altered ERK phosphorylation during T-cell RICD in the presence of TMPA or THPN (data not shown) and rapid Nur77 upregulation during T-cell RICD was not affected by TMPA or THPN. Thus, the reduced T-cell RICD in the presence of TMPA and THPN could not be explained by altered MEK/ERK signaling. While T-cell RICD was reduced, T-cell *intrinsic* TNFα and IFNγ production following *in vitro* re-stimulation were not significantly affected in both primary human and murine T-cell blasts by TMPA. Presence *vs.* absence of TMPA during primary human T-cell expansion did not affect its anti-apoptotic potential during T-cell re-stimulation. However, we observed reduced primary proliferation of mature T-cells in the presence of higher doses of TMPA and THPN. Nur77 is also rapidly upregulated during primary T-cell activation (data not shown), however we have not yet addressed whether the observed anti-proliferative effects of higher concentrations of TMPA or THPN occur Nur77-dependently.

4.3 Dual function of TMPA in mature T-cell RICD

Since we have observed counterintuitive anti-apoptotic effects of the Nur77 binding compounds THPN and TMPA on T-cell RICD, it was important to clarify, whether this effect was Nur77-dependent. Transcriptional profiling by RNA sequencing and analysis of RICD in Nur77 competent *vs.* deficient murine LCMV-specific T-cell blasts revealed both, Nur77-dependent but also Nur77-independent effects of these small molecule compounds during T-cell RICD. A graphical summary assembling Nur77-independent *vs.* dependent functions of Nur77-LBD binding compounds is depicted in **Figure 14** and **Figure 15**.

4.3.1 Nur77-independent impairment of T-cell RICD

Nur77 has been consistently reported as inductor of cell death in various solid tumor types like colon-, gastric-, pancreatic-, breast- or lung tumors even with predictive survival correlation *in vivo*[101,121,126,127,175]. The anti-tumor function of Nur77 targeting small molecule compounds has been demonstrated to depend on direct binding to the Nur77 LBD.

Our experimental data suggest a Nur77-independent T-cell RICD-reducing effect of these compounds (summarized in **Figure 14**). In line with the previously reported inconspicuous

phenotype of Nur77 deficient mice regarding activation induced T-cell apoptosis[81,154], genetic absence of T-cell *intrinsic* Nur77 did not affect T-cell RICD in mature murine T-cell blasts. In addition, siRNA knockdown of Nur77 in mature human T-cell blasts did similarly also not affect T-cell RICD. Still, TMPA reduced T-cell RICD, however similarly in Nur77 competent *vs.* deficient T-cell blasts. A functional redundancy between NR4A family members regarding T-cell apoptosis has been reported, especially between the highly homologous proteins Nur77 and Nor1[105,154]. Our experimental evidence suggests the presence of a Nur77-independent target for TMPA/THPN in mature T-cells undergoing RICD (**Figure 14**). Since we have demonstrated that Nor1 up-regulation is (non-significantly) augmented in Nur77 deficient T-cell blasts, these findings would be consistent with functional redundancy between Nur77 and Nor1. However, preliminary experiments using a combined siRNA mediated knockdown of Nur77 plus Nor1 argued against a compensating role of Nor1 during human T-cell RICD in Nur77 deficient T-cell blasts (data not shown). An alternative hypothesis to explain our experimental data would be that Nur77 binding small molecules interact with other, NR4A family non-related proteins involved in apoptosis. This alternative hypothesis is experimentally supported by the evidence that TMPA did not alter MOMP during T-cell RICD while caspase 9 showed a reduced activity in the presence of TMPA. Preliminary experimental evidence in favor of the latter hypothesis is that TMPA inhibited primary T-cell apoptosis induced by the indolcarbazole staurosporine, which occurs in the absence of Nur77 and Nor1 induction (data not shown). A potential non-NR4A family target for TMPA, based on these experimental results, could be a direct inhibitor of activated caspase 9 such as XIAP[188], a constitutively expressed anti-apoptotic regulator protein encoded by the *BIRC4* gene. Further investigation will address whether TMPA alters XIAP expression during T-cell RICD and whether the anti-apoptotic effects of TMPA depend on XIAP expression (**Figure 14**).

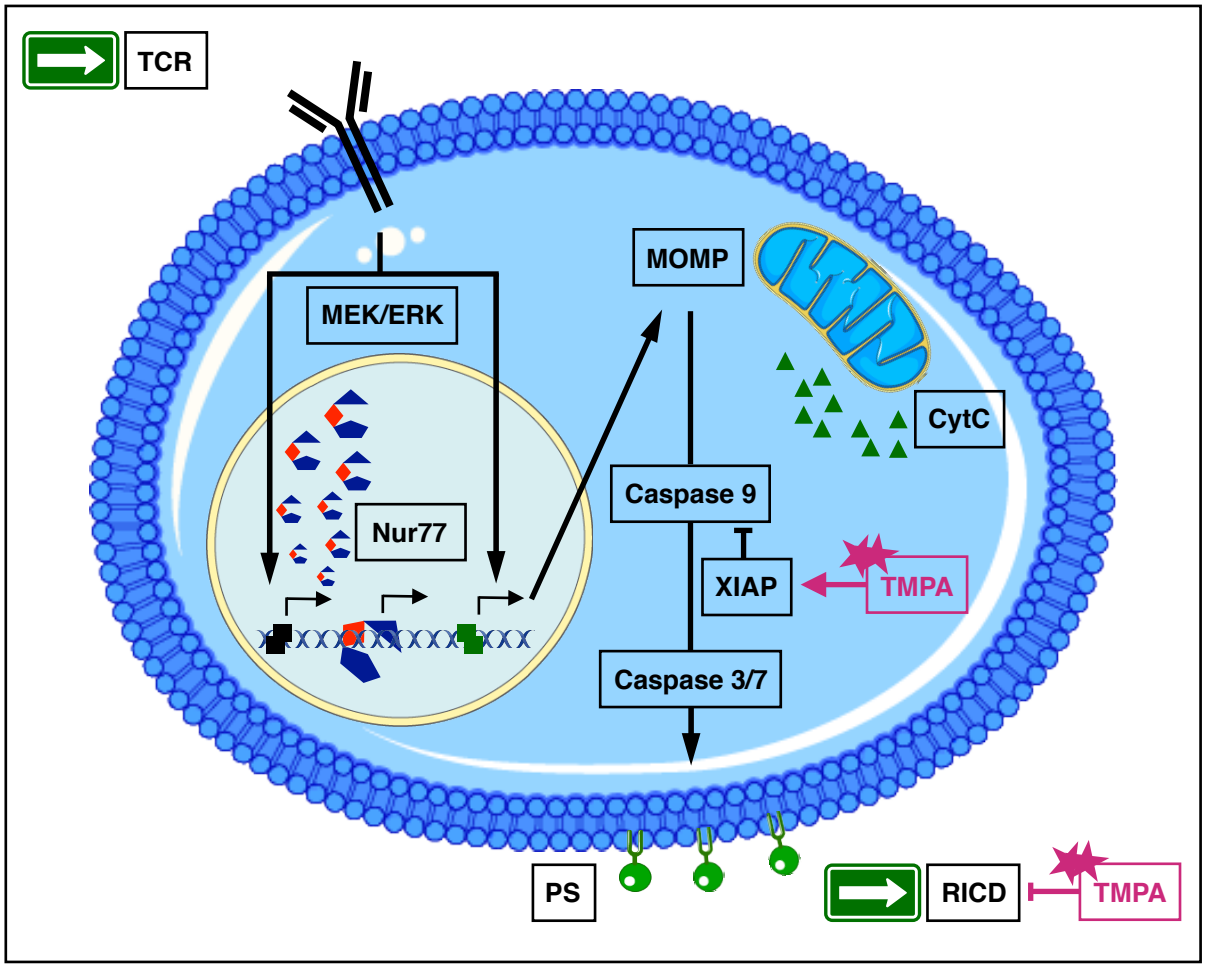

Figure 14 Nur77-independent impact of TMPA on RICD in primary mature T-cells
PS – phosphatidylserine, CytC – cytochrome C, MOMP – mitochondrial outer membrane permeabilization, → activating function, ⊣ inhibiting function, ↱ gene induction

4.3.2 Nur77-dependent regulation of *Sh2d1a*

Very early studies of Nur77 in TCR-mediated apoptosis have reported a crucial role of Nur77 transcription activity, that strictly correlated with its pro-apoptotic function, even *in vivo*[187]. In addition, overexpression and knockout systems of Nur77 in various solid tumor cell lines demonstrated consistent evidence of Nur77 to regulate apoptosis by *de novo* gene induction *via* its transcriptional activity[101,120,175,189]. Based on the experimental evidence of TMPA to reduce RICD in a Nur77-independent manner, we therefore compared transcriptional profiles during T-cell RICD in the presence *vs.* absence of TMPA. RNA sequencing using transgenic LCMV-specific murine T-cell blasts uncovered a set of 41 genes, that were significantly differentially regulated in a TMPA-dependent manner during T-cell RICD. Notably, 10% of these genes consisted of members of the Slamf receptor signaling axis, including the receptors Slamf1 (*Slamf1*), Slamf6 (*Slamf6*) and the intracellular adapter proteins SAP (*Sh2d1a*) and EAT2 (*Sh2d1b1*). SAP is an intracellular adapter protein of the costimulatory Slamf1- and Slamf6 receptor signaling axis, and is predominantly expressed in T- and natural killer (NK-) cells, whereas it is not expressed in B cells. Loss of function mutations in

the SAP encoding gene *SH2D1A* cause x-linked lymphoproliferative disease (XLP)[176,177,190]. In XLP patients, clinical phenotypes like severe infectious mononucleosis, lymphoproliferation and lymphoma as well as hypogammaglobulinemia are typically triggered by EBV infection, while no increased susceptibility against other pathogens has been reported. Importantly, RICD has been reported to be impaired in SAP deficient T-cells[66] similar to our results using TMPA in SAP competent T-cell blasts.

Re-stimulation of Nur77 competent *vs.* deficient primary murine T-cell blasts demonstrated that the TMPA-dependent down-regulation of *Sh2d1a* mRNA during RICD occurred only in Nur77 competent cells and was obviously not compensated by Nor1 expression (summarized in **Figure 15**).

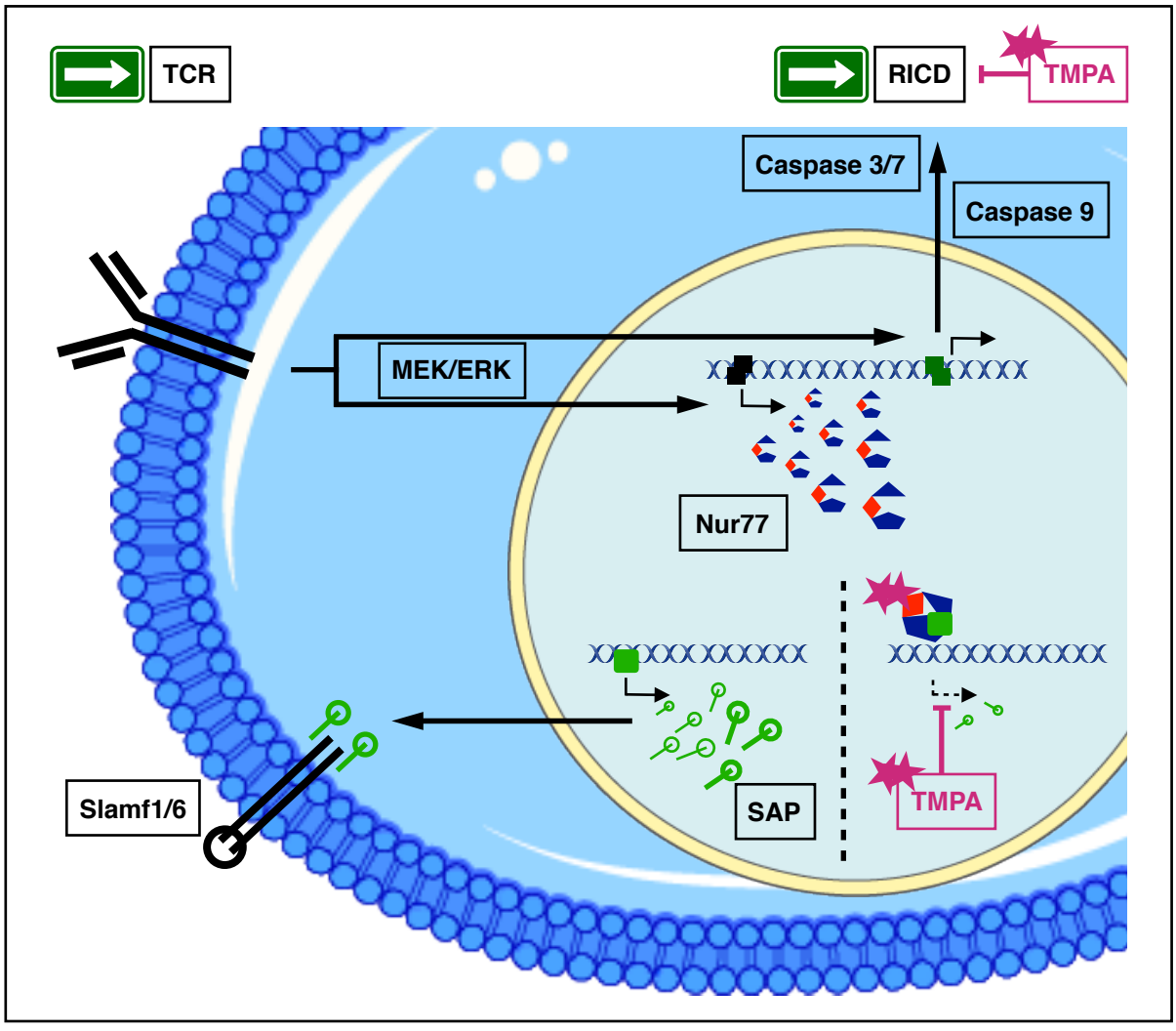

Figure 15 Nur77-dependent impact of TMPA on RICD in primary mature T-cells
activating function, inhibiting function, gene induction

4.4 Potential clinical application of Nur77 binding small molecule compounds

Our data demonstrate evidence for Nur77 binding small molecule compounds to reduce T-cell RICD. These compounds, designed to specifically bind to the unique hydrophobic LBD of the constitutive active transcription factor Nur77, reduced T-cell RICD Nur77-independently and modified *Sh2d1a* transcription in a Nur77-dependent manner.

The Nur77-independent molecular target of TMPA and THPN, respectively, remains to be defined. Our data suggest a target acting within the *intrinsic* apoptosis pathway downstream of the mitochondria, since MOMP was unaffected, whereas activation of caspase 9 was reduced in the presence of TMPA during T-cell RICD. XIAP could be a clinically relevant target, since its deficiency causes XLP-2 [188], a rare PID clinically rather similar to XLP-1. If TMPA would indeed increase or stabilize XIAP function, it would represent a personalized compound to enhance the function of hypomorphic XIAP mutations. The TMPA mediated, Nur77-dependent downregulation of SAP could also be used therapeutically. SAP has been described to support T helper-cell dependent antibody formation *in vivo*[191]. As this includes SAP mediated support of autoantibody formation[192,193], therapeutic reduction of SAP expression by TMPA related compounds could be used to lower auto-antibody production in autoimmune diseases. In addition, since SAP deficient T-cells show enhanced survival[66], TMPA could be used during T-cell-dependent vaccinations (e.g. against HIV[194]) or adoptive T-cell transfer to treat tumors[195].

A very attractive use of the Nur77 binding small molecule compounds studied in this thesis would be to treat cancer by induction of Nur77-dependent apoptosis in cancer cells[101,121,143,162,175] and at the same time to reduce RICD of cancer-specific T-cells. Whether such a dual-acting 'super-compound' fulfills its promises has to be tested in *in vivo* models of T-cell controlled tumors. A pharmacological reduction of T-cell RICD could also potentially improve treatment success in combination with checkpoint inhibitors during cancer therapy[196,197,198]. It is important to state that the *in vivo* application of Nur77 binding small molecule compounds may induce pleiotropic immunologic phenotypes. While early studies claimed, that mice lacking Nur77 did not have any immunological phenotype[81,148,154], more recent studies demonstrated Nur77 to regulate other important immunological functions in both lymphoid and myeloid cells. The development of Ly6C^{low} monocytes occurs Nur77-dependently and these cells orchestrate the monitoring and disposal of endothelial cells to control atherosclerosis[199,200]. In addition, caspase-independent cell death in macrophages was shown to depend on Nur77 [201,202]. More recent studies reported a role of Nur77 and Nor1 as suppressors of acute myeloid leukemia and myelodysplastic syndromes[105,106]. Also, the thymic development of regulatory T-cells is under the control of NR4A family proteins[203–

[205]. Still, TMPA has been applied *in vivo* and has not been described to cause toxicity[96]. Our plan is to titrate TMPA during acute and chronic murine infection with LCMV, a poorly-cytopathic virus controlled by $CD8^+$ T-cells[206]. A great advantage is, that the immune-control of LCMV is very well studied and tools to track virus-specific B- and T-cells exist[207]. *In vivo* use of TMPA, if used in human clinical trials, will require close monitoring of EBV replication, since it will be likely to induce a TMPA-dependent transient SAP deficiency[177]. Finally, the reported relevance of the NR4A receptors in chronic inflammatory diseases[208] such as chronic arthritis[209] and inflammation associated fibrosis[210] point to the need for long term *in vivo* monitoring of the immunologic and other effects of Nur77 LBD binding compounds.

5 Appendix

To this thesis, I attach my first authorship publication with the title "***Detection of Sp110 by Flow Cytometry and Application to Screening Patients for Veno-occlusive Disease with Immunodeficiency.***", published in the ***Journal of Clinical Immunology*** in **2017**.

6 References

1. Murphy, K. M. *Janeway's Immunobiology, 8th edition*. (Garland Science, Taylor & Francis Group, 2012).
2. Murphy, K. & Weaver, C. *Janeway's Immunobiology, 9th edition*. (Garland Science, Taylor & Francis Group, 2017).
3. Galluzzi, L. *et al.* Essential versus accessory aspects of cell death: Recommendations of the NCCD 2015. *Cell Death and Differentiation* **22,** 58–73 (2015).
4. Galluzzi, L., Bravo-San Pedro, J. M., Kepp, O. & Kroemer, G. Regulated cell death and adaptive stress responses. *Cellular and Molecular Life Sciences* **73,** 2405–2410 (2016).
5. Conrad, M., Angeli, J. P. F., Vandenabeele, P. & Stockwell, B. R. Regulated necrosis: Disease relevance and therapeutic opportunities. *Nature Reviews Drug Discovery* **15,** 348–366 (2016).
6. Weinlich, R., Oberst, A., Beere, H. M. & Green, D. R. Necroptosis in development, inflammation and disease. *Nature Reviews Molecular Cell Biology* **18,** 127–136 (2017).
7. Fuchs, Y. & Steller, H. Live to die another way: Modes of programmed cell death and the signals emanating from dying cells. *Nature Reviews Molecular Cell Biology* **16,** 329–344 (2015).
8. Pasparakis, M. & Vandenabeele, P. Necroptosis and its role in inflammation. *Nature* **517,** 311–320 (2015).
9. Nagata, S. & Golstein, P. The Fas Death Factor. *Science (80-.).* **267,** 1449–1456 (1995).
10. Lynch, D. H., Ramsdell, F. & Alderson, M. R. Fas and FasL in the homeostatic regulation of immune responses. *Immunol. Today* **16,** 569–74 (1995).
11. Burger, M. L., Leung, K. K., Bennett, M. J. & Winoto, A. T cell-specific inhibition of multiple apoptotic pathways blocks negative selection and causes autoimmunity. *Elife* **3,** 1–22 (2014).
12. West, A. P. & Shadel, G. S. Mitochondrial DNA in innate immune responses and inflammatory pathology. *Nature Reviews Immunology* **17,** 363–375 (2017).
13. Krysko, D. V. *et al.* Immunogenic cell death and DAMPs in cancer therapy. *Nature Reviews Cancer* **12,** 860–875 (2012).
14. Galluzzi, L., Kepp, O. & Kroemer, G. Mitochondria: Master regulators of danger signalling. *Nature Reviews Molecular Cell Biology* **13,** 780–788 (2012).
15. McDonald, B. *et al.* Intravascular danger signals guide neutrophils to sites of sterile inflammation. *Science (80-.).* **330,** 362–366 (2010).
16. Schweichel, J. -U & Merker, H. -J. The morphology of various types of cell death in prenatal tissues. *Teratology* **7,** 253–266 (1973).
17. Galluzzi, L. *et al.* Cell death modalities: Classification and pathophysiological implications. *Cell Death and Differentiation* **14,** 1237–1243 (2007).
18. Galluzzi, L. *et al.* Molecular mechanisms of cell death: Recommendations of the Nomenclature Committee on Cell Death 2018. *Cell Death Differ.* **25,** 486–541 (2018).
19. Galluzzi, L. *et al.* Molecular definitions of cell death subroutines: Recommendations of the Nomenclature Committee on Cell Death 2012. *Cell Death and Differentiation* **19,** 107–120 (2012).
20. Kroemer, G. *et al.* Classification of cell death: Recommendations of the Nomenclature Committee on Cell Death 2009. *Cell Death and Differentiation* **16,** 3–11 (2009).
21. Galluzzi, L. *et al.* Guidelines for the use and interpretation of assays for monitoring cell death in higher eukaryotes. *Cell Death and Differentiation* **16,** 1093–1107 (2009).
22. Levine, B. L. *et al.* Effects of CD28 costimulation on long-term proliferation of CD4+ T cells in the absence of exogenous feeder cells. *J. Immunol.* **159,** 5921–5930 (1997).
23. Lenardo, M. *et al.* MATURE T LYMPHOCYTE APOPTOSIS—Immune Regulation in a

Dynamic and Unpredictable Antigenic Environment. *Annu. Rev. Immunol.* **17,** 221–253 (1999).
24. Ashwell, J. D., Longo, D. L. & Bridges, S. H. T-cell tumor elimination as a result of T-cell receptor-mediated activation. *Science* **237,** 61–64 (1987).
25. Ashwell, B. Y. J. D., Cunningham, R. E., Noguchi, P. D. & Hernandez, D. Cell growth cycle block of T cell hybridomas upon activation with antigen. *J. Exp. Med.* **165,** (1987).
26. Bouillet, P. & O'Reilly, L. A. CD95, BIM and T cell homeostasis. *Nature Reviews Immunology* **9,** 514–519 (2009).
27. Bidère, N., Su, H. C. & Lenardo, M. J. GENETIC DISORDERS OF PROGRAMMED CELL DEATH IN THE IMMUNE SYSTEM. *Annu. Rev. Immunol.* **24,** 321–352 (2006).
28. Duke, R. C. & Cohen, J. J. IL-2 addiction: withdrawal of growth factor activates a suicide program in dependent T cells. *Lymphokine research* **5,** 289–299 (1986).
29. Rodríguez-Tarduchy, G. & López-Rivas, A. Phorbol esters inhibit apoptosis in IL-2-dependent T lymphocytes. *Biochem. Biophys. Res. Commun.* **164,** 1069–1075 (1989).
30. Elmore, S. Apoptosis: A Review of Programmed Cell Death. *Toxicologic Pathology* **35,** 495–516 (2007).
31. Galluzzi, L., Kepp, O. & Kroemer, G. Mitochondrial regulation of cell death: a phylogenetically conserved control. *Microb. Cell* **3,** 101–108 (2016).
32. Tait, S. W. G. & Green, D. R. Mitochondria and cell death: outer membrane permeabilization and beyond. *Nat. Rev. Mol. Cell Biol.* **11,** 621–632 (2010).
33. Delbridge, A. R. D., Grabow, S., Strasser, A. & Vaux, D. L. Thirty years of BCL-2: Translating cell death discoveries into novel cancer therapies. *Nature Reviews Cancer* **16,** 99–109 (2016).
34. Luna-Vargas, M. P. A. & Chipuk, J. E. Physiological and Pharmacological Control of BAK, BAX, and Beyond. *Trends in Cell Biology* **26,** 906–917 (2016).
35. Aouacheria, A., Rech de Laval, V., Combet, C. & Hardwick, J. M. Evolution of Bcl-2 homology motifs: Homology versus homoplasy. *Trends in Cell Biology* **23,** 103–111 (2013).
36. Llambi, F. *et al.* BOK Is a Non-canonical BCL-2 Family Effector of Apoptosis Regulated by ER-Associated Degradation. *Cell* **165,** 421–433 (2016).
37. Edlich, F. *et al.* Bcl-xL retrotranslocates Bax from the mitochondria into the cytosol. *Cell* **145,** 104–116 (2011).
38. Kuwana, T. *et al.* BH3 domains of BH3-only proteins differentially regulate Bax-mediated mitochondrial membrane permeabilization both directly and indirectly. *Mol. Cell* **17,** 525–535 (2005).
39. Chen, L. *et al.* Differential targeting of prosurvival Bcl-2 proteins by their BH3-only ligands allows complementary apoptotic function. *Mol. Cell* **17,** 393–403 (2005).
40. Chen, H.-C. *et al.* An interconnected hierarchical model of cell death regulation by the BCL-2 family. *Nat. Cell Biol.* (2015). doi:10.1038/ncb3236
41. Dai, H., Pang, Y. P., Ramirez-Alvarado, M. & Kaufmann, S. H. Evaluation of the BH3-only protein Puma as a direct Bak activator. *J. Biol. Chem.* **289,** 89–99 (2014).
42. Moldoveanu, T. *et al.* BID-induced structural changes in BAK promote apoptosis. *Nat. Struct. Mol. Biol.* **20,** 589–597 (2013).
43. Dai, H. *et al.* Transient binding of an activator BH3 domain to the Bak BH3-binding groove initiates Bak oligomerization. *J. Cell Biol.* **194,** 39–48 (2011).
44. Ren, D. *et al.* BID, BIM, and PUMA are essential for activation of the BAX- and BAK-dependent cell death program. *Science (80-.).* **330,** 1390–1393 (2010).
45. Luo, X., Budihardjo, I., Zou, H., Slaughter, C. & Wang, X. Bid, a Bcl2 interacting protein, mediates cytochrome c release from mitochondria in response to activation of cell surface death receptors. *Cell* **94,** 481–490 (1998).
46. Czabotar, P. E., Lessene, G., Strasser, A. & Adams, J. M. Control of apoptosis by the BCL-2 protein family: Implications for physiology and therapy. *Nature Reviews Molecular Cell Biology* **15,** 49–63 (2014).
47. Moldoveanu, T., Follis, A. V., Kriwacki, R. W. & Green, D. R. Many players in BCL-2

family affairs. *Trends in Biochemical Sciences* **39,** 101–111 (2014).
48. Shamas-Din, A., Kale, J., Leber, B. & Andrews, D. W. Mechanisms of action of Bcl-2 family proteins. *Cold Spring Harb. Perspect. Biol.* **5,** 1–21 (2013).
49. Li, P. *et al.* Cytochrome c and dATP-dependent formation of Apaf-1/caspase-9 complex initiates an apoptotic protease cascade. *Cell* **91,** 479–489 (1997).
50. Jiang, X. J. & Wang, X. D. Cytochrome C-mediated apoptosis. *Annu. Rev. Biochem.* **73,** 87–106 (2004).
51. Chai, J. *et al.* Structural and biochemical basis of apoptotic activation by Smac/DIABLO. *Nature* **406,** 855–862 (2000).
52. Verhagen, A. M. *et al.* Identification of DIABLO, a mammalian protein that promotes apoptosis by binding to and antagonizing IAP proteins. *Cell* **102,** 43–53 (2000).
53. Du, C., Fang, M., Li, Y., Li, L. & Wang, X. Smac, a mitochondrial protein that promotes cytochrome c-dependent caspase activation by eliminating IAP inhibition. *Cell* **102,** 33–42 (2000).
54. Salvesen, G. S. & Duckett, C. S. IAP proteins: Blocking the road to death's door. *Nature Reviews Molecular Cell Biology* **3,** 401–410 (2002).
55. Eckelman, B. P. & Salvesen, G. S. The human anti-apoptotic proteins cIAP1 and cIAP2 bind but do not inhibit caspases. *J. Biol. Chem.* **281,** 3254–3260 (2006).
56. Eckelman, B. P., Salvesen, G. S. & Scott, F. L. Human inhibitor of apoptosis proteins: Why XIAP is the black sheep of the family. *EMBO Rep.* **7,** 988–994 (2006).
57. Kischkel, F. C. *et al.* Cytotoxicity-dependent APO-1 (Fas/CD95)-associated proteins form a death-inducing signaling complex (DISC) with the receptor. *EMBO J.* **14,** 5579–88 (1995).
58. Slape, C. I. *et al.* Inhibition of apoptosis by BCL2 prevents leukemic transformation of a murine myelodysplastic syndrome. *Blood* **120,** 2475–2483 (2012).
59. Morris, G., Walker, A. J., Berk, M., Maes, M. & Puri, B. K. Cell Death Pathways: a Novel Therapeutic Approach for Neuroscientists. *Mol. Neurobiol.* 1–20 (2017). doi:10.1007/s12035-017-0793-y
60. Meythaler, M. *et al.* Differential CD4+ T-lymphocyte apoptosis and bystander T-cell activation in rhesus macaques and sooty mangabeys during acute simian immunodeficiency virus infection. *J. Virol.* **83,** 572–83 (2009).
61. Groux, H. *et al.* Activation-induced death by apoptosis in CD4+ T cells from human immunodeficiency virus-infected asymptomatic individuals. *J Exp Med* **175,** 331–340 (1992).
62. Zhao, B. Bin *et al.* T Lymphocytes from Chronic HCV-Infected Patients Are Primed for Activation-Induced Apoptosis and Express Unique Pro-Apoptotic Gene Signature. *PLoS One* **8,** (2013).
63. Chhabra, A., Mehrotra, S., Chakraborty, N. G., Dorsky, D. I. & Mukherji, B. Activation-induced cell death of human melanoma specific cytotoxic T lymphocytes is mediated by apoptosis-inducing factor. *Eur. J. Immunol.* **36,** 3167–3174 (2006).
64. Nabhani, S. *et al. Deregulation of Fas ligand expression as a novel cause of autoimmune lymphoproliferative syndrome-like disease*. *Haematologica* **100,** (2015).
65. Price, S. *et al.* Natural history of autoimmune lymphoproliferative syndrome associated with FAS gene mutations. *Blood* **123,** 1989–1999 (2014).
66. Snow, A. L. *et al.* Restimulation-induced apoptosis of T cells is impaired in patients with X-linked lymphoproliferative disease caused by SAP deficiency. *J Clin. Investig.* **119,** (2009).
67. Katz, G., Krummey, S. M., Larsen, S. E., Stinson, J. R. & Snow, A. L. SAP Facilitates Recruitment and Activation of LCK at NTB-A Receptors during Restimulation-Induced Cell Death. *J. Immunol.* **192,** 4202–4209 (2014).
68. Larsen, S. E. *et al.* Sensitivity to Restimulation-Induced Cell Death Is Linked to Glycolytic Metabolism in Human T Cells. *J. Immunol.* **198,** 147–155 (2017).
69. Hansen, A., Lipsky, P. E. & D??rner, T. B-cell lymphoproliferation in chronic inflammatory rheumatic diseases. *Nature Clinical Practice Rheumatology* **3,** 561–569 (2007).

70. Mulay, S. R. *et al.* Central role of defective apoptosis in autoimmunity. *Nat. Commun.* **7,** 10274 (2016).
71. Prasad, K. V. & Prabhakar, B. S. Apoptosis and autoimmune disorders. *Autoimmunity* **36,** 323–330 (2003).
72. Barrionuevo-Cornejo, C. & Dueñas-Hancco, D. Lymphadenopathies in human immunodeficiency virus infection. *Semin. Diagn. Pathol.* **35,** 84–91 (2017).
73. Carbone, A. & Gloghini, A. AIDS-related lymphomas: From pathogenesis to pathology. *British Journal of Haematology* **130,** 662–670 (2005).
74. Sen, R. & Baltimore, D. Inducibility of kappa immunoglobulin enhancer-binding protein Nf-kappa B by a posttranslational mechanism. *Cell* **47,** 921–8 (1986).
75. Lane, D. P. & Crawford, L. V. T antigen is bound to a host protein in SV40-transformed cells. *Nature* **278,** 261–263 (1979).
76. Chawta, A., Repa, J. J., Evans, R. M. & Mangelsdorf, D. J. Nuclear receptors and lipid physiology: Opening the x-files. *Science* **294,** 1866–1870 (2001).
77. Kliewer, S. A., Lehmann, J. M. & Willson, T. M. Orphan nuclear receptors: Shifting endocrinology into reverse. *Science* **284,** 757–760 (1999).
78. Germain, P., Staels, B., Dacquet, C., Spedding, M. & Laudet, V. Overview of Nomenclature of Nuclear Receptors. *Pharmacol. Rev.* **58,** 685–704 (2006).
79. Mangelsdorf, D. J. *et al.* The nuclear receptor superfamily: the second decade. *Cell* **83,** 835–839 (1995).
80. Maxwell. The NR4A subgroup: immediate early response genes with pleiotropic physiological roles. *Nucl. Recept. Signal.* **4,** (2006).
81. Lee, S. L. *et al.* Unimpaired thymic and peripheral T cell death in mice lacking the nuclear receptor NGFI-B (Nur77). *Science* **269,** 532–535 (1995).
82. Woronicz, J. D., Calnan, B., Ngo, V. & Winoto, A. Requirement for the orphan steroid receptor Nur77 in apoptosis of T-cell hybridomas. *Nature* **367,** 277–81 (1994).
83. Gruber, F. *et al.* Direct binding of Nur77/NAK-1 to the plasminogen activator inhibitor 1 (PAI-1) promoter regulates TNFα-induced PAI-1 expression. *Blood* **101,** 3042–3048 (2003).
84. Martin, L. J. & Tremblay, J. J. The human 3β-hydroxysteroid dehydrogenase/Δ5- Δ4 isomerase type 2 promoter is a novel target for the immediate early orphan nuclear receptor Nur77 in steroidogenic cells. *Endocrinology* **146,** 861–869 (2005).
85. Pei, L. *et al.* NR4A orphan nuclear receptors are transcriptional regulators of hepatic glucose metabolism. *Nat. Med.* **12,** 1048–1055 (2006).
86. Woronicz, J. D. *et al.* Regulation of the Nur77 orphan steroid receptor in activation-induced apoptosis. *Mol. Cell. Biol.* **15,** 6364–76 (1995).
87. Masuyama, N. *et al.* Akt Inhibits the Orphan Nuclear Receptor Nur77 and T-cell Apoptosis. *J. Biol. Chem.* **276,** 32799–32805 (2001).
88. Martínez-González, J. & Badimon, L. The NR4A subfamily of nuclear receptors: New early genes regulated by growth factors in vascular cells. *Cardiovascular Research* **65,** 609–618 (2005).
89. Okabe, T. *et al.* cDNA cloning of a NGFI-B/nur77-related transcription factor from an apoptotic human T cell line. *J. Immunol.* **154,** 3871–9 (1995).
90. Wilson, T. E., Fahrner, T. J., Johnston, M. & Milbrandt, J. Identification of the DNA binding site for NGFI-B by genetic selection in yeast. *Science* **252,** 1296–1300 (1991).
91. Philips, a *et al.* Novel dimeric Nur77 signaling mechanism in endocrine and lymphoid cells. *Mol. Cell. Biol.* **17,** 5946–5951 (1997).
92. Chintharlapalli, S. *et al.* Activation of Nur77 by selected 1,1-bis(3′-indolyl)-1-(p-substituted phenyl)methanes induces apoptosis through nuclear pathways. *J. Biol. Chem.* **280,** 24903–24914 (2005).
93. Zhan, Y. *et al.* Cytosporone B is an agonist for nuclear orphan receptor Nur77. *Nat. Chem. Biol.* **4,** 548–56 (2008).
94. Wang, W. *et al.* Orphan nuclear receptor TR3 acts in autophagic cell death via mitochondrial signaling pathway. *Nat. Chem. Biol.* **10,** 133–140 (2013).
95. Wang, W. J. *et al.* Induction of Autophagic Death in Cancer Cells by Agonizing TR3

and Attenuating Akt2 Activity. *Chem. Biol.* **22,** 1040–1051 (2015).
96. Zhan, Y. *et al.* The orphan nuclear receptor Nur77 regulates LKB1 localization and activates AMPK. *Nat. Chem. Biol.* **8,** (2012).
97. Li, Q.-X., Ke, N., Sundaram, R. & Wong-Staal, F. NR4A1, 2, 3--an orphan nuclear hormone receptor family involved in cell apoptosis and carcinogenesis. *Histol. Histopathol.* **21,** 533–540 (2006).
98. Moll, U. M., Marchenko, N. & Zhang, X. K. p53 and Nur77/TR3 - Transcription factors that directly target mitochondria for cell death induction. *Oncogene* **25,** 4725–4743 (2006).
99. Liu, S. *et al.* Norcantharidin induces melanoma cell apoptosis through activation of TR3 dependent pathway. *Cancer Biol. Ther.* **12,** 1005–1014 (2011).
100. Smith, A. G., Lim, W., Pearen, M., Muscat, G. E. O. & Sturm, R. A. Regulation of NR4A nuclear receptor expression by oncogenic BRAF in melanoma cells. *Pigment Cell Melanoma Res.* **24,** 551–563 (2011).
101. Yu, H., Kumar, S. M., Fang, D., Acs, G. & Xu, X. Nuclear orphan receptor TR3/Nur77 mediates melanoma cell apoptosis. *Cancer Biol. Ther.* **6,** 405–412 (2007).
102. Chen, J. *et al.* Cotreatment with BCL-2 antagonist sensitizes cutaneous T-cell lymphoma to lethal action of HDAC7-Nur77-based mechanism. *Blood* **113,** 4038–4048 (2009).
103. Deutsch, A. J. A. *et al.* NR4A1-mediated apoptosis suppresses lymphomagenesis and is associated with a favorable cancer-specific survival in patients with aggressive B-cell lymphomas. *Blood* **123,** 2367–2377 (2014).
104. Liu, H. B. *et al.* The anti-leukemic effect of a novel histone deacetylase inhibitor MCT-1 and 5-aza-cytidine involves augmentation of Nur77 and inhibition of MMP-9 expression. *Int. J. Oncol.* **34,** 573–579 (2009).
105. Mullican, S. E. *et al.* Abrogation of nuclear receptors Nr4a3 and Nr4a1 leads to development of acute myeloid leukemia. *Nat. Med.* **13,** 730–735 (2007).
106. Ramirez-Herrick, A. M., Mullican, S. E., Sheehan, A. M. & Conneely, O. M. Reduced NR4A gene dosage leads to mixed myelodysplastic/myeloproliferative neoplasms in mice. *Blood* **117,** 2681–2690 (2011).
107. Zhou, L. *et al.* HDAC inhibition by SNDX-275 (Entinostat) restores expression of silenced leukemia-associated transcription factors Nur77 and Nor1 and of key pro-apoptotic proteins in AML. *Leukemia* **27,** 1358–1368 (2013).
108. Li, Y. *et al.* Molecular determinants of AHPN (CD437)-induced growth arrest and apoptosis in human lung cancer cell lines. *Mol. Cell. Biol.* **18,** 4719–31 (1998).
109. Xia, Z. *et al.* Relative impact of 3- and 5-hydroxyl groups of cytosporone B on cancer cell viability. *Med. Chem. Commun.* **4,** 332–339 (2013).
110. Uemura, H. & Chang, C. Antisense TR3 orphan receptor can increase prostate cancer cell viability with etoposide treatment. *Endocrinology* **139,** 2329–2334 (1998).
111. Mu, X. & Chang, C. TR3 Orphan Nuclear Receptor Mediates Apoptosis through Up-regulating E2F1 in Human Prostate Cancer LNCaP Cells. *J. Biol. Chem.* **278,** 42840–42845 (2003).
112. Yu, L., Su, Y. S., Zhao, J., Wang, H. & Li, W. Repression of NR4A1 by a chromatin modifier promotes docetaxel resistance in PC-3 human prostate cancer cells. *FEBS Lett.* **587,** 2542–2551 (2013).
113. Gimmi, C. D. *et al.* Breast cancer-associated antigen, DF3/MUC1, induces apoptosis of activated human T cells. *Nat. Med.* **2,** 1367–1370 (1996).
114. Ye, X. *et al.* Distinct role and functional mode of TR3 and RARalpha in mediating ATRA-induced signalling pathway in breast and gastric cancer cells. *Int J Biochem Cell Biol* **36,** 98–113 (2004).
115. Kolluri, S. K. *et al.* A Short Nur77-Derived Peptide Converts Bcl-2 from a Protector to a Killer. *Cancer Cell* **14,** 285–298 (2008).
116. Sibayama-Imazu, T. *et al.* Induction of apoptosis in PA-1 ovarian cancer cells by vitamin K 2 is associated with an increase in the level of TR3/Nur77 and its accumulation in mitochondria and nuclei. *J. Cancer Res. Clin. Oncol.* **134,** 803–812

(2008).
117. Sun, Z. *et al.* Inhibition of B-catenin signaling by nongenomic action of orphan nuclear receptor Nur77. *Oncogene* **31,** 2653–2667 (2012).
118. Lin, X.-F. RXR acts as a carrier for TR3 nuclear export in a 9-cis retinoic acid-dependent manner in gastric cancer cells. *J. Cell Sci.* **117,** 5609–5621 (2004).
119. Wu, Q., Liu, S., Ye, X., Huang, Z. & Su, W. Dual roles of Nur77 in selective regulation of apoptosis and cell cycle by TPA and ATRA in gastric cancer cells. *Carcinogenesis* **23,** 1583–1592 (2002).
120. Wilson, A. J. *et al.* TR3 modulates platinum resistance in ovarian cancer. *Cancer Res.* **73,** 4758–4769 (2013).
121. Sung, D. C. *et al.* Nur77 agonists induce proapoptotic genes and responses in colon cancer cells through nuclear receptor-dependent and nuclear receptor-independent pathways. *Cancer Res.* **67,** 674–683 (2007).
122. Cho, S. D. *et al.* Activation of nerve growth factor-induced B alpha by methylene-substituted diindolylmethanes in bladder cancer cells induces apoptosis and inhibits tumor growth. *Mol. Pharmacol.* **77,** 396–404 (2010).
123. To, S. K. Y., Zeng, W. J., Zeng, J. Z. & Wong, A. S. T. Hypoxia triggers a Nur77-β-catenin feed-forward loop to promote the invasive growth of colon cancer cells. *Br. J. Cancer* **110,** 935–945 (2014).
124. Schumacker, P. T. Hypoxia-inducible factor-1 (HIF-1). *Critical Care Medicine* **33,** (2005).
125. Choi, J. W., Park, S. C., Kang, G. H., Liu, J. O. & Youn, H. D. Nur77 Activated by Hypoxia-Inducible Factor-1α Overproduces Proopiomelanocortin in von Hippel-Lindau-Mutated Renal Cell Carcinoma. *Cancer Res.* **64,** 35–39 (2004).
126. Lee, S.-O. *et al.* The nuclear receptor TR3 regulates mTORC1 signaling in lung cancer cells expressing wild-type p53. *Oncogene* **31,** 3265–3276 (2012).
127. Muscat, G. E. O. *et al.* Research Resource: Nuclear Receptors as Transcriptome: Discriminant and Prognostic Value in Breast Cancer. *Mol. Endocrinol.* **27,** 350–365 (2013).
128. Kolesar, J. M. *et al.* Vorinostat in combination with bortezomib in patients with advanced malignancies directly alters transcription of target genes. *Cancer Chemother. Pharmacol.* **72,** 661–667 (2013).
129. Cory, S. & Adams, J. M. The BCL2 family: Regulators of the cellular life-or-death switch. *Nature Reviews Cancer* **2,** 647–656 (2002).
130. Hill, M. M., Adrain, C., Duriez, P. J., Creagh, E. M. & Martin, S. J. Analysis of the composition, assembly kinetics and activity of native Apaf-1 apoptosomes. *EMBO J.* **23,** 2134–2145 (2004).
131. Saelens, X. *et al.* Toxic proteins released from mitochondria in cell death. *Oncogene* **23,** 2861–2874 (2004).
132. Seger, R. & Krebs, E. G. The MAPK signaling cascade. *Faseb J* **9,** 726–735 (1995).
133. Kim, H. J. *et al.* α-lipoic acid prevents neointimal hyperplasia via induction of p38 mitogen-activated protein kinase/Nur77-mediated apoptosis of vascular smooth muscle cells and accelerates postinjury reendothelialization. *Arterioscler. Thromb. Vasc. Biol.* **30,** 2164–2172 (2010).
134. Liu, P. Y. *et al.* Expression of Nur77 induced by an n-butylidenephthalide derivative promotes apoptosis and inhibits cell growth in oral squamous cell carcinoma. *Invest. New Drugs* **30,** 79–89 (2012).
135. Yang, H., Nie, Y., Li, Y. & Wan, Y. J. Y. ERK1/2 deactivation enhances cytoplasmic Nur77 expression level and improves the apoptotic effect of fenretinide in human liver cancer cells. *Biochem. Pharmacol.* **81,** 910–916 (2011).
136. Chen, H. Z. *et al.* Prolyl isomerase Pin1 stabilizes and activates orphan nuclear receptor TR3 to promote mitogenesis. *Oncogene* **31,** 2876–2887 (2012).
137. Fresno Vara, J. a *et al.* PI3K/Akt signalling pathway and cancer. *Cancer Treat. Rev.* **30,** 193–204 (2004).
138. Huo, J., Xu, S. & Lam, K. P. Fas apoptosis inhibitory molecule regulates T cell

receptor-mediated apoptosis of thymocytes by modulating akt activation and Nur77 expression. *J. Biol. Chem.* **285,** 11827–11835 (2010).
139. Lammi, J. & Aarnisalo, P. FGF-8 stimulates the expression of NR4A orphan nuclear receptors in osteoblasts. *Mol. Cell. Endocrinol.* **295,** 87–93 (2008).
140. Han, Y.-H. *et al.* Regulation of Nur77 nuclear export by c-Jun N-terminal kinase and Akt. *Oncogene* **25,** 2974–2986 (2006).
141. Kiss, I. *et al.* Adenosine A2Areceptor-mediated cell death of mouse thymocytes involves adenylate cyclase and Bim and is negatively regulated by Nur77. *Eur. J. Immunol.* **36,** 1559–1571 (2006).
142. Rajpal, A. *et al.* Transcriptional activation of known and novel apoptotic pathways by Nur77 orphan steroid receptor. *EMBO J.* **22,** 6526–36 (2003).
143. Lin, B. *et al.* Conversion of Bcl-2 from Protector to Killer by Interaction with Nuclear Orphan Receptor Nur77/TR3. *Cell* **116,** 527–540 (2004).
144. Zhang, J. *et al.* Receptor-mediated apoptosis in T lymphocytes. in *Cold Spring Harbor Symposia on Quantitative Biology* **64,** 363–371 (1999).
145. Liu, Z. G., Smith, S. W., McLaughlin, K. A., Schwartz, L. M. & Osborne, B. A. Apoptotic signals delivered through the T-cell receptor of a T-cell hybrid require the immediate-early gene nur77. *Nature* **367,** 281–4 (1994).
146. Calnan, B. J., Szychowski, S., Chan, F. K., Cado, D. & Winoto, A. A role for the orphan steroid receptor Nur77 in apoptosis accompanying antigen-induced negative selection. *Immunity* **3,** 273–82 (1995).
147. Suzuki, A. *et al.* T cell-specific loss of Pten leads to defects in central and peripheral tolerance. *Immunity* **14,** 523–534 (2001).
148. Zhou, T. *et al.* Inhibition of Nur77/Nurr1 leads to inefficient clonal deletion of self-reactive T cells. *J. Exp. Med.* **183,** 1879–92 (1996).
149. Kang, H. J. *et al.* Retinoic acid and its receptors repress the expression and transactivation functions of Nur77: A possible mechanism for the inhibition of apoptosis by retinoic acid. *Exp. Cell Res.* **256,** 545–554 (2000).
150. Katagiri, Y. *et al.* Modulation of retinoid signalling through NGF-induced nuclear export of NGFI-B. *Nat. Cell Biol.* **2,** 435–440 (2000).
151. Cunningham, N. R. *et al.* Immature CD4+CD8+ Thymocytes and Mature T Cells Regulate Nur77 Distinctly in Response to TCR Stimulation. *J. Immunol.* **177,** 6660–6666 (2006).
152. Amsen, D., Revilla Calvo, C., Osborne, B. a & Kruisbeek, a M. Costimulatory signals are required for induction of transcription factor Nur77 during negative selection of CD4(+)CD8(+) thymocytes. *Proc. Natl. Acad. Sci. U. S. A.* **96,** 622–7 (1999).
153. Feske, S., Giltnane, J., Dolmetsch, R., Staudt, L. M. & Rao, A. Gene regulation mediated by calcium signals in T lymphocytes. *Nat. Immunol.* **2,** 316–324 (2001).
154. Cheng, L. E. C., Chan, F. K. M., Cado, D. & Winoto, A. Functional redundancy of the Nur77 and Nor-1 orphan steroid receptors in T-cell apoptosis. *EMBO J.* **16,** 1865–1875 (1997).
155. Ranhotra, H. S. The NR4A orphan nuclear receptors: Mediators in metabolism and diseases. *Journal of Receptors and Signal Transduction* **35,** 184–188 (2015).
156. Mohan, H. M. *et al.* Molecular pathways: The role of NR4A orphan nuclear receptors in cancer. *Clin. Cancer Res.* **18,** 3223–3228 (2012).
157. Winoto, A. & Littman, D. R. Review Nuclear Hormone Receptors in T Lymphocytes. *Cell* **109,** 5766 (2002).
158. Hsu, H.-C., Zhou, T. & Mountz, J. D. Nur77 family of nuclear hormone receptors. *Curr. Drug Targets. Inflamm. Allergy* **3,** 413–23 (2004).
159. Liu, S. *et al.* Induction of apoptosis by TPA and VP-16 is through translocation of TR3. *World J. Gastroenterol.* **8,** 446–450 (2002).
160. Liu, J. *et al.* Modulation of orphan nuclear receptor Nur77-mediated apoptotic pathway by acetylshikonin and analogues. *Cancer Res.* **68,** 8871–8880 (2008).
161. Chen, H. Z. *et al.* Akt phosphorylates the TR3 orphan receptor and blocks its targeting to the mitochondria. *Carcinogenesis* **29,** 2078–2088 (2008).

162. Liu, J. J. *et al.* A unique pharmacophore for activation of the nuclear orphan receptor Nur77 in vivo and in vitro. *Cancer Res.* **70,** 3628–3637 (2010).
163. Pawlak, A., Strzadala, L. & Kalas, W. Non-genomic effects of the NR4A1/Nur77/TR3/NGFIB orphan nuclear receptor. *Steroids* **95,** 1–6 (2015).
164. Pircher, HP, Moskophidis, D, Rohrer U, Bürki, K, Hengartner, H, Zinkernagel, R. Viral escape by selection of cytotoxic T cell-resistant virus variants in vivo. *Nature* **1,** 15796–15799 (1990).
165. Pircher, H. *et al.* Characterization of virus-specific cytotoxic T cell clones from allogeneic bone marrow chimeras. *Eur J Immunol* **17,** 159–66. (1987).
166. Pircher, H. *et al.* Molecular analysis of the antigen receptor of virus-specific cytotoxic T cells and identification of a new V alpha family. *Eur J Immunol* **17,** 1843–1846 (1987).
167. Vermes, I., Haanen, C., Steffens-Nakken, H. & Reutellingsperger, C. A novel assay for apoptosis Flow cytometric detection of phosphatidylserine expression on early apoptotic cells using fluorescein labelled Annexin V. *J. Immunol. Methods* **184,** 39–51 (1995).
168. Pfaffl, M. W. A new mathematical model for relative quantification in real-time RT-PCR. *Nucleic Acids Res.* **29,** 45e–45 (2001).
169. Zhou, Y. H. Pathway analysis for RNA-Seq data using a score-based approach. *Biometrics* **72,** 165–174 (2016).
170. Fu, Y., Luo, L., Luo, N., Zhu, X. & Garvey, W. T. NR4A orphan nuclear receptors modulate insulin action and the glucose transport system: potential role in insulin resistance. *J. Biol. Chem.* **282,** 31525–31533 (2007).
171. Frayn, K. N., Karpe, F., Fielding, B. A., Macdonald, I. A. & Coppack, S. W. Integrative physiology of human adipose tissue. *International Journal of Obesity* **27,** 875–888 (2003).
172. Duncia, J. V. *et al.* MEK inhibitors: The chemistry and biological activity of U0126, its analogs, and cyclization products. *Bioorganic Med. Chem. Lett.* **8,** 2839–2844 (1998).
173. Squires, M. S., Nixon, P. M. & Cook, S. J. Cell-cycle arrest by PD184352 requires inhibition of extracellular signal-regulated kinases (ERK) 1/2 but not ERK5/BMK1. *Biochem. J.* **366,** 673–680 (2002).
174. Luciano, F. *et al.* Nur77 converts phenotype of Bcl-B, an antiapoptotic protein expressed in plasma cells and myeloma. *Blood* **109,** 3849–3855 (2007).
175. Wilson, A. J., Arango, D., Mariadason, J. M., Heerdt, B. G. & Augenlicht, L. H. TR3/Nur77 in colon cancer cell apoptosis. *Cancer Res.* **63,** 5401–5407 (2003).
176. Schuster, V. & Kreth, H. W. X-linked lymphoproliferative disease is caused by deficiency of a novel SH2 domain-containing signal transduction adaptor protein. *Immunol. Rev.* **178,** 21–8 (2000).
177. Tangye, S. G. XLP: Clinical Features and Molecular Etiology due to Mutations in SH2D1A Encoding SAP. *Journal of Clinical Immunology* **34,** 772–779 (2014).
178. Hazel, T. G., Nathans, D. & Lau, L. F. A gene inducible by serum growth factors encodes a member of the steroid and thyroid hormone receptor superfamily. *Proc. Natl. Acad. Sci. U. S. A.* **85,** 8444–8 (1988).
179. Milbrandt, J. Nerve growth factor induces a gene homologous to the glucocorticoid receptor gene. *Neuron* **1,** 183–188 (1988).
180. Wang, Z. *et al.* Structure and function of Nurr1 identifies a class of ligand-independent nuclear receptors. *Nature* **423,** 555–560 (2003).
181. Codina, A. *et al.* Identification of a novel co-regulator interaction surface on the ligand binding domain of Nurr1 using NMR footprinting. *J. Biol. Chem.* **279,** 53338–53345 (2004).
182. Zhang, X. Targeting Nur77 translocation. *Expert Opin. Ther. Targets* **11,** 69–79 (2007).
183. Safe, S., Jin, U.-H., Hedrick, E., Reeder, A. & Lee, S.-O. Minireview: role of orphan nuclear receptors in cancer and potential as drug targets. *Mol. Endocrinol.* **28,** 157–72 (2014).
184. Davis, I. J., Hazel, T. G., Chen, R. H., Blenis, J. & Lau, L. F. Functional domains and

phosphorylation of the orphan receptor Nur77. *Mol. Endocrinol.* **7,** 953–964 (1993).
185. Wang, A., Rud, J., Olson, C. M., Anguita, J. & Osborne, B. A. Phosphorylation of Nur77 by the MEK-ERK-RSK Cascade Induces Mitochondrial Translocation and Apoptosis in T Cells. *J. Immunol.* **183,** 3268–3277 (2009).
186. Jacobs, C. M., Boldingh, K. A., Slagsvold, H. H., Thoresen, G. H. & Paulsen, R. E. ERK2 prohibits apoptosis-induced subcellular translocation of orphan nuclear receptor NGFI-B/TR3. *J. Biol. Chem.* **279,** 50097–50101 (2004).
187. Kuang, A. A., Cado, D. & Winoto, A. Nur77 transcription activity correlates with its apoptotic function in vivo. *Eur. J. Immunol.* **29,** 3722–8 (1999).
188. Marsh, R. A. *et al.* XIAP deficiency: A unique primary immunodeficiency best classified as X-linked familial hemophagocytic lymphohistiocytosis and not as X-linked lymphoproliferative disease. *Blood* **116,** 1079–1082 (2010).
189. Lee, S.-O. *et al.* Diindolylmethane Analogs Bind NR4A1 and Are NR4A1 Antagonists in Colon Cancer Cells. *Mol. Endocrinol.* **28,** 1729–1739 (2014).
190. Malbran, A., Belmonte, L., Ruibal-Ares, B., Bare, P. & Bracco, M. M. [X-linked lymphoproliferative syndrome, EBV virus infection and defects in cytotoxicity lymphocyte regulation]. *Med. (B Aires)* **63,** 70–76 (2003).
191. Crotty, S., Kersh, E. N., Cannons, J., Schwartzberg, P. L. & Ahmed, R. SAP is required for generating long-term humoral immunity. *Nature* **421,** 282–287 (2003).
192. Sawada, S. *et al.* SLAM-associated protein solves a mystery of autoimmunity. in *Annals of the New York Academy of Sciences* **1109,** 19–30 (2007).
193. Sawada, S. Slam-associated protein plays a key role in development of autoimmunity. *Autoimmunity Reviews* **11,** 804–805 (2012).
194. Vaccine, H.-. Lessons Learned in Developing a Commercial FIV Vaccine: The Immunity Required for an Effective HIV-1 Vaccine. *Viruses* 10–12 (2018). doi:10.3390/v10050277
195. Arvind, C. Mitochondria-centric activation induced cell death of cytolytic T lymphocytes and its implications for cancer immunotherapy. *Vaccine* **28,** 4566–4572 (2010).
196. Márquez-Rodas, I. *et al.* Immune checkpoint inhibitors: therapeutic advances in melanoma. *Ann. Transl. Med.* **3,** 267 (2015).
197. Teply, B. A. & Lipson, E. J. Identification and management of toxicities from immune checkpoint-blocking drugs. *Oncology (Williston Park).* **28,** 1–12 (2014).
198. Villadolid, J. & Amin, A. Immune checkpoint inhibitors in clinical practice: update on management of immune-related toxicities. *Transl. Lung Cancer Res.* **4,** 560–575 (2015).
199. Carlin, L. M. *et al.* Nr4a1-dependent Ly6Clow monocytes monitor endothelial cells and orchestrate their disposal. *Cell* **153,** 362–375 (2013).
200. Hanna, R. N. *et al.* The transcription factor NR4A1 (Nur77) controls bone marrow differentiation and the survival of Ly6C- monocytes. *Nat. Immunol.* **12,** 778–785 (2011).
201. Kim, S. O., Ono, K., Tobias, P. S. & Han, J. Orphan Nuclear Receptor Nur77 Is Involved in Caspase-independent Macrophage Cell Death. *J. Exp. Med.* **197,** 1441–1452 (2003).
202. Zhang, L., Xie, F., Zhang, J., Dijke, P. ten & Zhou, F. SUMO-triggered ubiquitination of NR4A1 controls macrophage cell death. *Cell Death Differ.* **24,** 1530–1539 (2017).
203. Tao, R. & Hancock, W. W. Resistance of Foxp3+ regulatory T cells to Nur77-induced apoptosis promotes allograft survival. *PLoS One* **3,** (2008).
204. Fassett, M. S., Jiang, W., D'Alise, A. M., Mathis, D. & Benoist, C. Nuclear receptor Nr4a1 modulates both regulatory T-cell (Treg) differentiation and clonal deletion. *Proc. Natl. Acad. Sci.* **109,** 3891–3896 (2012).
205. Sekiya, T. *et al.* Nr4a receptors are essential for thymic regulatory T cell development and immune homeostasis. *Nat Immunol* **14,** 230–237 (2013).
206. Oldstone, M. B. A. A suspenseful game of 'hide and seek' between virus and host. *Nat. Immunol.* **8,** 325–327 (2007).
207. Zhou, X., Ramachandran, S., Mann, M. & Popkin, D. L. Role of lymphocytic

choriomeningitis virus (LCMV) in understanding viral immunology: Past, present and future. *Viruses* **4,** 2650–2669 (2012).
208. McMorrow, J. P. & Murphy, E. P. Inflammation: a role for NR4A orphan nuclear receptors? *Biochem. Soc. Trans.* **39,** 688–693 (2011).
209. De Silva, S. *et al.* Reduction of the incidence and severity of collagen-induced arthritis by constitutive Nur77 expression in the T cell lineage. *Arthritis Rheum.* **52,** 333–338 (2005).
210. Palumbo-Zerr, K. *et al.* Orphan nuclear receptor NR4A1 regulates transforming growth factor-β signaling and fibrosis. *Nat. Med.* **21,** 150–158 (2015).